Operando spectroscopies and heterogeneous olefin polymerization catalysis: A rare marriage with a lot of potential beyond usual understanding

Elena Groppo [a,*], Alessandro Piovano [a,b]

[a] *Department of Chemistry, NIS Centre and INSTM, University of Torino, via Giuria 7, 10125 Turin, Italy*
[b] *GAME Lab, Department of Applied Science and Technology, Polytechnic of Torino, Corso Duca Degli Abruzzi 24, 10129 Torino, Italy*

ARTICLE INFO

ABSTRACT

This short review summarizes the main results achieved in the field of *operando* spectroscopies applied to heterogeneous catalysts for olefin polymerization. Following a chronological order, starting from the first spectroscopic measurements applied to the Phillips catalyst, the review retraces the main stages of this exciting story, reporting also some details on the experimental set-ups adopted from time to time, the difficulties encountered, the failures, and the solutions taken to address the problems. What emerges is a dynamic picture with still many unexplored potentialities, even though unfortunately limited to a few research groups systematically engaged in this field.

1. Introduction

1.1. Context and challenges

Polyolefins (POs) are irreplaceable materials in every days life. The secret behind their success story lies in their extremely high versatility, both in terms of properties and applications [1–13]. Entangling just a single type of monomer (ethylene or propylene) it is possible to obtain thousands of different materials, with very different properties in terms of, e.g., crystallinity, chain regularity, morphology, and mechanical behaviour. This explains why, born as plastic commodities (especially in the packaging sector, enabling safe supply of food and medicine), today POs are increasingly used as lightweight engineering plastics for automotive and architectural applications, textiles, rubbers, and for electrical and thermal insulation. Opposite to the most common perception, POs meet the demand for sustainability [14–16]. When compared to other commonly used plastics, POs rank well in terms of adherence to green design principles, determined using metrics such as atom economy, mass from renewable sources, biodegradability, percent recycled, distance of furthest feedstock, price, life cycle health hazards and life cycle energy use. PO polymers exhibit 100% atom economy (i.e. their production does not generate waste), one among the highest rate of recycling, the lowest price, and negligible toxicity. More important, the life-cycle environmental impacts of POs production, assessed using Life Cycle Analysis (LCA) methodology, is the lowest among the most

common plastics, with low greenhouse gas emissions ("carbon footprint"), low weight, and high versatility. This is entirely due to the highly energy-, resource- and atom- efficient processes which are used for their production.

In particular, the key of such efficient production processes is constituted by the use of appropriate catalysts, belonging to three main classes: the heterogeneous Phillips and Ziegler-Natta catalysts, and the homogeneous molecular catalysts (based on metallocene complexes and analogues). The three classes of catalysts satisfy different needs of the market, and hence they should be considered complementary, rather than competing to each other. Olefin polymerization catalysts are probably the most efficient catalysts employed in the chemical industry, with turnover frequencies (TOFs) competing with the efficiency of enzymes optimized in thousands of years by Nature. Sufficient to say that these catalysts are so efficient that the minor amount of residues which remain inside the polymer do not need to be removed. As such, they represent a unique exception in industrial catalysis, because they are not recovered at the end of the reaction, but remain embedded in the produced polymer. This is guaranteed by the rapid and efficient fragmentation of the catalysts particles during the polymerization reaction. Indeed, formation of solid polymer at the active sites of the catalyst induces a stress which cause the support to disintegrate into smaller fragments. Along this process, new active sites are continuously exposed to the incoming monomer. This prevents mass transfer limitation and pore blocking, and allows to sustain (or even increase) the catalyst

activity [17,18].

Despite nearly 80 years of history, POs are materials in constant evolution. Among the main challenges, there is the ability to control the molecular architecture (e.g. number and position of branching, stereo-regularity, block copolymers etc.) and polymer morphology (structure of the granules, crystals, nanostructure). Moreover, extending the lifetime of POs, as well as introducing functional groups in the otherwise non polar polymer chains, would represent two real steps forward circularity in plastic economy, because it would allow POs to replace high performance thermoplastic materials in many engineering applications. Ultimately, this would allow the production of all-polyolefin composite materials, which is one of the key-point to enable a facile polymer recycling, by both mechanical and chemical routes [13,19].

These challenges can only be addressed by carefully working on the catalysts and the olefin polymerization technology. In particular, catalysts for the polymerization of olefins are placed at the heart of POs production. Catalysts optimization requires the fundamental understanding of their physical-chemical properties, the elucidation of the active sites structure, the ability do discriminate between active, spectator and dormant sites and the understanding of the intimate relationship between active sites, activator, monomer and growing polymer chains, to name just a few of the fundamental issues in this field. Potentially, *operando* spectroscopies can help in answering these questions. However, opposite to many other fields in heterogeneous catalysis, the marriage between olefin polymerization catalysis and *operando* spectroscopies has been quite rare so far. Very few research groups in the world have systematically applied *operando* spectroscopies to the study of olefin polymerization catalysts. Some of the reasons behind this fact are summarized in the following.

1. *Need of a chemical activation*. First of all, the active sites are generated upon activation of a precatalyst. Differently from the majority of heterogeneous catalysts, which are activated through a "simple" thermal activation in a well-defined atmosphere, olefin polymerization catalysts usually require a chemical activation, which may be achieved by the reaction with the olefins themselves or by the use of Al-alkyl activators (or their derivatives). In both cases, the main effect of the activation is the alkylation of the metal centre, generating a metal-alkyl bond which is considered the active site for olefin insertion. The problem is that this step is very delicate and harshly sensitive to the presence of moisture, quite difficult to be carried out in a research laboratory otherwise devoted to spectroscopic characterization. On the other hand, researchers with competencies and skills for this kind of industrial plants and protocols usually do not have experience at all in spectroscopy. Bridging this gap is not straightforward and requires the development of dedicated experimental set-ups. Measurements which are considered ordinary in many fields of catalysis are not so in this field and usually much more time and energy consuming.

2. *Poor stability of the active sites*. The so generated active sites are extremely reactive and suffer for rapid deactivation, especially in the absence of the monomer and/or of the solvent. For example, the metal-alkyl bond originated by the reaction of the metal precursor with the Al-alkyl activator may rapidly undergo β-H elimination with the consequent formation of an inactive metal-hydride. Moreover, the metal is susceptible to over-reduction when the activator is used in large excess, which is however a common practice in a polymerisation reactor, where a fraction of the Al-alkyl acts as scavenger of moisture impurities, rather than as activator. This means that in most of the cases the activation of the precatalyst should be performed in stoichiometric amount and in the presence of the monomer or just before its entrance in the reactor, which are all additional complications from an experimental point of view.

3. *Scarce accessibility of the active sites*. The active sites are often scarcely accessible, because they remain in interaction with the activator or its by-products. This is exemplified by the formation of ion-pairs between activated metallocene complexes and methylalumoxane (MAO) [5,20,21], but it is common also in Ziegler-Natta catalysis where the Al-alkyl chloride (or similar) by-products may remain in close proximity of the Ti-alkyl sites [22], and recently demonstrated to occur also for the Phillips catalyst (vide infra) [23,24]. The poor accessibility of the active sites makes the use of spectroscopy of (insertion) probe molecules much more challenging than for many other heterogeneous catalysts.

4. *The solid polymer remains at the catalyst surface*. In the presence of the monomer, the catalyst particles are very rapidly embedded in the formed polymer, thus hiding the working catalytic sites from the spectroscopic measurement. As a matter of fact, while in the industrial reactors the polymerization is so impetuous to induce the fragmentation of the catalyst particles (thus continuously exposing new catalytic sites to the reaction environment), in the spectroscopic cells the polymerization conditions are usually much milder and not sufficient to induce that fragmentation. Besides being detrimental for the catalyst activity, in most of the cases this represents a strong limitation for optical spectroscopies. As a matter of fact, the thick polymer layer surrounding the catalyst particles not only completely changes their scattering properties, but also masks the active sites, preventing (or at least limiting) their detection.

5. *Exothermicity of the reaction*. Olefin polymerization is strongly exothermic. In an industrial polymerization reactor, the generated heat is removed through different technological solutions. However, this is not easy to be pursued in a reactor designed for spectroscopic measurements. As a consequence, the spectroscopic results may be affected by the rapid over-heating of the sample. A local temperature increase may cause the partial melting of the polymer layer around the catalyst particles, and consequently diffusion limitation for the incoming monomer.

1.2. The concept of operando spectroscopy applied to olefin polymerization: a semantic issue

Despite the difficulties discussed above, several examples of *operando* spectroscopies applied to heterogeneous olefin polymerization catalysts can be found in the literature. Before starting to summarize some of the main results achieved in this field, it is important to clarify what does *operando* approach mean in the field of olefin polymerization catalysis, and the difference with respect to *in situ* spectroscopic measurements. As a matter of fact, the use of the term *operando* referring to spectroscopic measurements on polymerization catalysts is quite controversial.

According to the definition coined by Miguel Banares at the beginning of 2000 [25–27], the *operando* methodology indicates that the catalyst characterization is performed under working conditions (as close as possible to the industrial reaction conditions) and is combined with simultaneous measurement of catalytic activity and/or selectivity. When activity is not evaluated, the term *in situ* is more appropriate. In the majority of cases, the reactants and products are in the gas phase, and normally the outlet product stream is monitored by gas chromatography or mass spectrometry, so that conversion and/or selectivity can be determined simultaneously to the spectroscopic measurements. Clearly, this is not possible when the product is a solid, which does not leave the reaction cell but remains on the catalyst. In polymerization catalysis, the concepts of activity and selectivity themselves are different and more complex to be defined with respect to many other gas-phase catalytic processes. Activity is defined in terms of productivity, i.e. how many grams of polymer are produced per grams of catalyst per hour, rather than in terms of conversion. As far as selectivity is concerned, it depends on the type of polymer. When referring to polyethylene, the two most relevant parameters affecting the selectivity are the melt index, which reflects the average molecular weight of the polymer chains, and the polymer density, which is a function of its crystallinity degree. While for polypropylene, selectivity is usually referred to the isotacticity index, which indicates the fraction of isotactic

polymer and is usually measured by determining the fraction of the polymer insoluble in boiling heptane.

These considerations imply that in olefin polymerization catalysis activity and selectivity cannot be evaluated with a single measurement, but require the adoption of different instrumentations, which are not compatible with the *operando* approach in its classical definition. Does this mean that it is not possible to perform *operando* spectroscopic measurements on these catalysts? This topic was a subject of debate at the recent *7th International Congress on Operando Spectroscopy* congress at Grindelwald (CH), and the majority of the scientific community spoke in favour of the fact that the discriminating factor to define whether or not a spectroscopic measurement is *operando*, is the ability to monitor the formation of the product, i.e. the polymer, during the spectroscopic experiment: whenever the growing polymer product is quantified and/ or characterized during the spectroscopic measurement, then the experiment can be defined as *operando*.

Potentially, both IR and DR UV-Vis-NIR spectroscopies applied to heterogenous olefin polymerization catalysts in the presence of the monomer might allow to quantify the growing polymer as a function of time, i.e. to obtain information on the polymerization rate. In fact, the vibrational manifestations of the growing polymer are easily distinguishable from the vibrations of the catalyst itself, both in the Mid-IR and in the Near-IR regions: monitoring the intensity of these bands as a function of time allows to determine the catalyst activity. On the other hand, the number and position of the bands characteristic of the polymer allows to characterize some of its properties, e.g. the crystallinity or the branching degree, which allow us to talk about selectivity. In particular, focusing on the simplest polyolefin (polyethylene), the catalyst "precision" is measured in terms of ability to provide specific molecular weight distribution and to incorporate comonomers in such a way to achieve an even distribution of short branching. Some of this information can be retrieved by the vibrational features of the growing polymer. Finally, a through analysis of the vibrational spectra collected during the polymerization might allow to detect reaction intermediates useful to highlight the reaction mechanism and eventually the occurrence of cooperative phenomena involving more than one type of active sites.

As far as the reactor cells are concerned, the gap with respect to the industrial reactors is less pronounced than in many other fields in catalysis. Insertion olefin polymerization occurs at very mild conditions (atmospheric pressure and temperature below 100 °C), not so far from those achievable in spectroscopic reactors. On this basis, time-resolved IR and DR UV-Vis-NIR (and to some extent also X-ray absorption) experiments performed on heterogeneous olefin polymerization catalysts in the presence of the monomer should be defined as *operando* without hesitation, just as experiments conducted on other types of heterogeneous catalysts, where not only the reactants but also the products are in the gas phase, and hence detectable outstream by analytical methods.

1.3. Structure of the review

In this review we will provide several examples of the potential of this *operando* spectroscopic approach applied to heterogenous olefin polymerization catalysts. According to the definition discussed above, we will focus the attention exclusively on spectroscopic data collected in the presence of the monomer and/or of the co-catalyst, while we will skip the multitude of results obtained through *in situ* spectroscopic methods. However, it is important to mention that *in situ* spectroscopic measurements, often performed in the presence of different types of probe molecules, as well as theoretical calculation, also played (and still play) a major role in the understanding of olefin polymerization catalysts at a molecular level.

The paper is organized according to a sort of chronological order. Chapter two is devoted to the Phillips catalyst, which was the first olefin polymerization catalyst to be investigated by means of *operando* spectroscopies, mainly due to the simplicity of the catalyst formulation. In Chapter 3 Al-alkyls, used as activators in the great majority of cases,

enter the scene. It is thus the turn of *operando* spectroscopies applied to Ziegler-Natta (ZN) catalysts, where most of the successful stories regard the elucidation of the effects of the activator on the pre-catalysts. Chapter 4 is entirely dedicated to the potential of *operando* IR spectroscopy in determining the kinetics of olefin polymerization, in evaluating the relative amount of accessible sites and their inherent ability in inserting the olefin monomer into the metal-alkyl bond. Finally, Chapter 5 describes the role of *operando* IR spectroscopy in unravelling synergistic phenomena occurring between different types of active sites in the same catalyst. The different experimental set-ups and strategies developed by different research groups are also briefly discussed in each chapter. Final remarks and perspectives are discussed in Chapter 6.

2. Early stages of ethylene polymerization on the Phillips catalyst

2.1. Ethylene polymerization mechanism on the CO-reduced Cr(II)/SiO$_2$ catalyst

2.1.1. An historical challenge

For many years after the onset of the *operando* concept, in the field of olefin polymerization catalysis *operando* spectroscopies were almost exclusively applied to the investigation of the Phillips catalyst, especially the CO-reduced one, where the chromium sites are in the Cr(II) reduced form [28–35]. In fact, this catalytic system is one of the few olefin polymerization catalyst that does not require the use of any Al-alkyl activator to develop activity in ethylene polymerization, but it is activated by ethylene itself in the first stages of the catalytic process. For the CO-reduced Cr(II)/SiO$_2$ catalyst the ethylene polymerization reaction occurs at very mild conditions (sub-atmospheric pressure of ethylene, room temperature or even below) almost without any induction time (typically required in the case of oxidized Cr(VI)/SiO$_2$ catalyst). For this reason, it can be monitored easily using standard spectroscopic cells, provided that they allow thermal treatments at high temperature (higher than 600 °C) in both oxidizing and reducing atmosphere, which is a necessary condition to activate correctly the catalyst, avoiding segregation of a fraction of the chromium sites in the form of inactive Cr$_2$O$_3$ particles (vide infra) [30,32,35]. According to the experience of the authors, quartz cells are by far the most reliable ones, whereas cells containing metallic components, including most of the commercially available cells for performing *operando* IR, UV-Vis and XAS spectroscopy, inevitably suffer of some drawbacks.

Historically, one of the questions that mostly triggered the scientific community was the identification of the initiation mechanism of the ethylene polymerization [28–30,32,33,36]. Indeed, the highly diluted Cr(II) sites present at the surface of amorphous silica do not have any alkyl ligand, hence ethylene itself should be responsible for the formation of the first Cr-R active sites. Several mechanisms were proposed in the past to account for Cr(II) alkylation by ethylene (also called Cr(II) self-alkylation), which are strictly connected with the question on the nature of the chromium active sites and their oxidation state [30,33, 37–50]. However, a clearcut identification of the key intermediates by *operando* spectroscopies is still missing. One of the main difficulties is the very small fraction of the active sites. Typically, the total amount of chromium does not exceed 1 wt%, but it is commonly accepted that only some percentage of the total chromium sites display activity, while the others behave, at best, as dormant sites [28–31]. This means that, whichever is the technique of choice to identify the active sites, it must be sensitive enough, but also "selective", i.e. able to discriminate between active, inactive and/or dormant species [34,51].

2.1.2. Direct detection of Cr-alkyl key-intermediates by operando IR spectroscopy

By far, *operando* IR spectroscopy has been the mostly used technique to address the challenge of detecting Cr-alkyl key intermediates in a direct way, with the purpose of validating and/or disproving the

initiation mechanism proposed in the literature. Fig. 1A shows the typical experimental set-up used in our laboratory, which was developed by Zecchina in the late 1960s and is still in use today, almost unaltered. The catalyst is placed inside a quartz cell equipped with KBr windows, which can be connected to a vacuum line system for sending ethylene, while simultaneously collecting the IR spectra. Prior the polymerization experiment, the catalyst is activated in the same cell, and no more exposed to moisture. The reaction can be performed in a variable temperature range from -180 °C to room temperature and, with some modification of the cell, also up to 150 °C. IR spectroscopy is potentially able to discriminate between different Cr-alkyl key-intermediates on the basis of their vibrational properties, in particular in the region of CH_x vibrational modes. The main obstacle is represented by the extremely rapid polymerization rate. According to Mc Daniel estimations, the typical TOF is as high as 5000 ethylene molecules inserted per site per second, that means that in 1 s a polymer chain as long as 10^4 CH_2 units might be formed per each site [30]. This means that, even using sub-second acquisition times, the IR spectra are invariably dominated by the fingerprint of the already long polymer chains [32,51–55]. This is shown in B, which reports a sequence of IR spectra collected in only 15 s during ethylene polymerization at room temperature on a CO-reduced $Cr(II)/SiO_2$ catalyst, in the $\nu(CHx)$ spectral region. The two bands at about 2920 and 2850 cm^{-1}, which constantly grow in intensity over time, are ascribed to the asymmetric and symmetric $\nu(CH_2)$ vibrational modes of PE, and no evidence of other absorption bands ascribable to shorter polymer chains and/or key-intermediates are observed, which is in agreement with the extremely high TOF values predicted by Mc Daniel [28–31].

In the attempt to freeze the key-intermediates formed during the early stages of the reaction, and to detect them by means of *operando* IR spectroscopy, two distinctly different approaches were pursued in the past. On one side, sequential small doses of ethylene were sent in the reaction cell [56]. This was useful to detect π-adsorbed ethylene on Cr (II) sites. These species, later on detected also by other authors, are relatively stable and hence not necessarily related to active sites only [55,57,58]. The second approach [55,59] consisted in lowering the polymerization rate. This is possible either by lowering the temperature, or by poisoning the catalyst, or by a combination of the two strategies. As an example, Fig. 1C shows a sequence of IR spectra collected starting from − 100 °C up to room temperature during the ethylene polymerization on a $Cr(II)/SiO_2$ catalyst [55,59]. At the very beginning (i.e. at the lowest temperature, spectrum 1), the spectrum is dominated by the

fingerprints of π-adsorbed ethylene on Cr(II) sites (band at 3004 cm^{-1}) [58]. Upon increasing temperature, a series of "anomalous" bands are observed in the CH_x stretching region (namely at 2965, 2931, 2915, 2893 and 2861 cm^{-1}), where the term "anomalous" indicates that they are not observed in the spectrum of polyethylene. These bands were assigned to the $\nu(CH_2)$ modes of small $(CH_2)_n$ cycles on the chromium sites (also called metallacycles), characterized by a structural strain which gradually decreases with increasing ring dimension. Similar bands were observed also when ethylene polymerization was performed on a $Cr(II)/SiO_2$ catalyst poisoned by CO, a molecule able to coordinate to the Cr(II) sites but less strongly than ethylene [59].

These "anomalous" IR absorption bands were taken as a demonstration of the occurrence of the so called "metallacycle" initiation mechanism, a two-electron redox process during which Cr(II) is oxidized to Cr(IV) by oxidative addition of ethylene. A similar mechanism is well-documented for selective oligomerization of ethylene to α-olefins on homogeneous chromium complexes [60–62]. However, recent theoretical calculation predicted unfeasibly high propagation barriers following this route [39–41]. This would suggest that Cr(IV)-metallacycle intermediates might be spectators rather than active species or that, once formed, chain propagation should occur following another mechanism and not the simple progressive enlargement of the metallacycle. Indeed, according to McGuinnes, chain propagation would follow the Cossee-Arlman mechanism [49]. In this respect, Scott and co-workers proposed that a Cr(IV)-cyclopentane may undergo a Cr−C bond homolysis assisted by a second Cr(II) site at the silica surface [41]. This implies a neat-one electron redox process, during which the Cr (IV)-cyclopentane intermediate is reduced to a Cr(III)-butyl radical that immediately reacts with the second Cr(II), generating a Cr (III)-butyl-Cr(III) species. Mc Daniel and co-workers, instead, proposed that a Cr(IV)-cycloheptyl ring or similar species may undergo H-transfer either to the Cr(IV) site itself or to the coordinated ethylene to give a Cr-H or Cr-ethyl species, which then would act as starting group for the first polymer chain [50]. According to this second hypothesis, the oxidation state of the chromium sites does not change, and remains Cr (IV).

2.1.3. Assessing the oxidation state of the chromium species by operando XANES and DR UV-Vis spectroscopies

It is evident that the problem of the self-alkylation mechanism of Cr (II) sites by ethylene cannot be solved by *operando* IR spectroscopy alone and that it is strictly related to the assessment of the oxidation state of
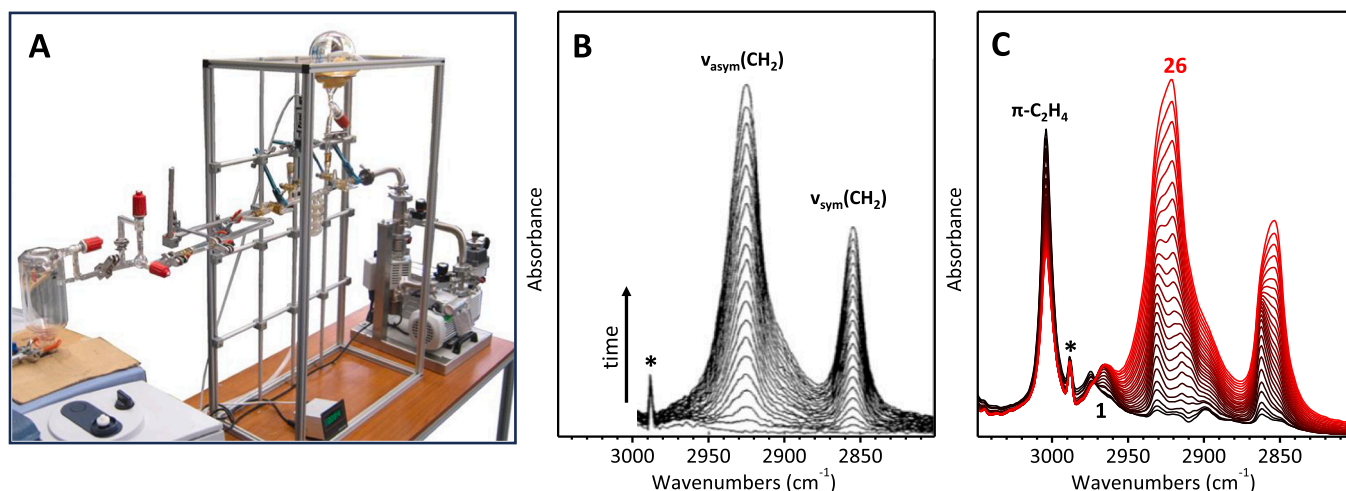

Fig. 1. Part A: Typical experimental set-up for performing operando IR spectroscopy during ethylene polymerization in the UNITO laboratories. The cell placed in the spectrophotometer is designed for measurements at variable temperature. Part B: Sequence of operando IR spectra, in the $\nu(CHx)$ region, collected every second during ethylene polymerization at room temperature on a CO-reduced $Cr(II)/SiO_2$ catalyst. [54] Part C: The same as in part B, for ethylene polymerization performed at variable temperature, from − 100 °C to room temperature (from spectrum 1 to 26), in order to decrease the reaction rate and hence increasing the probability to detect key intermediates. [59] The bands labelled with asterisks in Parts B and C are associated to gaseous ethylene.

the active chromium species, which is probably the most debated topic on this catalyst at present time [33]. UV-Vis and XANES spectroscopies have been probably the mostly used techniques to answer to this question, even though interpretation of results has been (and still is) object of discussion. Perhaps the first Cr K-edge XAS data on CO-reduced Cr (II)/SiO₂ catalysts were reported by Weckhuysen and co-workers in the late 1995 [63]. It was only ten years later that we performed the first, pioneering, *operando* Cr K-edge XANES experiment during ethylene polymerization on a CO-reduced Cr(II)/SiO₂ catalyst [64]. The experiment was accomplished on a 4 wt% Cr-loaded catalyst in order to allow measurements in transmission mode. The catalyst was placed in the form of self-standing pellet inside a stainless steel home-made cell (inset in Fig. 2A), allowing thermal treatments to be performed only up to 500 °C. At that time, this experimental set-up was at the state of the art in the field [65]. However, the combination of all these factors (chromium loading higher than 1 wt%, activation temperature lower than 600 °C, metallic cell) led to a poorly activated catalyst, which contained a relevant fraction of inactive Cr_2O_3 clusters beside the desired highly uncoordinated Cr(II) sites. This is evident by looking to the XANES spectrum collected before ethylene polymerization (spectrum 1 in Fig. 2A), which contains not only the spectroscopic fingerprint of the uncoordinated Cr(II) sites (shoulder at 5995 eV on the rising edge), but also those of clustered Cr_2O_3 (band at 5990 eV in the pre-edge and at 6008 eV in the white-line region). After ethylene polymerization at 100 °C (spectrum 2 in Fig. 2A), the band ascribed to Cr(II) sites decreases in intensity (without disappearing), demonstrating their involvement in the reaction. However, it was not possible to obtain relevant information on the local structure and oxidation state of the active chromium species, because of the copresence of Cr_2O_3 clusters. Even greater problems were faced by the same authors some years later when attempting a similar experiment in RefleXAFS mode on a planar model of the Phillips catalyst, in collaboration with the group of P. Thune [66].

Even though Cr K-edge XANES spectra of similar or even better activated Cr(II)/SiO₂ catalysts were published in the successive years [67,68], it was only almost fifteen years later [33] that a similar ethylene polymerization experiment was performed on a 1 wt% CO-reduced Cr(II)/SiO₂ catalyst (Fig. 2B), using a quartz capillary with a diameter of 1.5 mm as polymerization reactor, which was connected to a gas manifold allowing to flow different gas mixtures. At the outcome of the capillary, a mass spectrometer allowed to detect eventual gaseous reaction by-products (inset in Fig. 2B). The beam was vertically focused in order to fit the 1.5 mm capillary, and only 4 mm of sample in the capillary direction were accessible to the X-rays beam to guarantee sample homogeneity (for a total of 1.5×4.0 mm beam size). This experimental set-up allowed the collection of quick-XANES spectra in fluorescence mode in about 12 min, as a compromise between time-resolution and signal-to-noise ratio [69]. The use of a quartz reactor, coupled with the low chromium loading, allowed to properly activate the Cr(II)/SiO₂ catalyst, achieving 100% of highly uncoordinated Cr(II) sites.

The spectrum of the Cr(II)/SiO₂ sample before ethylene polymerization (spectrum 1 in Fig. 2B) is distinctly different from that reported in Fig. 2A, with a remarkably intense shoulder around 5995 eV, assigned to a Cr(1 s)→Cr($4p_z$) transition and thus considered the fingerprint of isolated Cr(II) sites [67,70], and with no evidences of Cr_2O_3 clusters. During ethylene polymerization at room temperature, the spectra gradually evolve from that characteristic of Cr(II) species to a final spectrum corresponding to more oxidized sites (from spectrum 3 to 5 in Fig. 2B). In particular: i) the edge shifts at higher energy (from 6000 to 6002.5 eV, evaluated at the maximum of the derivative signals); ii) the shoulder at 5995 eV decreases in intensity and is gradually substituted by a new peak at 5993 eV, accounting for a total intensity of about 0.2 (in normalized absorption units). The observation of a pre-edge peak with non negligible intensity in the spectra of the sample during ethylene polymerization suggests that at least a fraction of the chromium sites have a symmetry characterized by an almost complete absence of the inversion centre. The occurrence of ethylene polymerization was testified not only by a change in the color of the sample (from light blue to white), but also by the observation that a successive re-activation treatment in oxygen at 650 °C produced CO and CO_2 in large amount, as detected by mass spectrometry. To date, this is probably the most elegant *operando* Cr K-edge XANES experiment performed during ethylene polymerization on a Cr(II)/SiO₂ catalyst. However, this experiment alone is scarcely informative on the nature of the active species, due to the well-known intrinsic difficulty of the method to
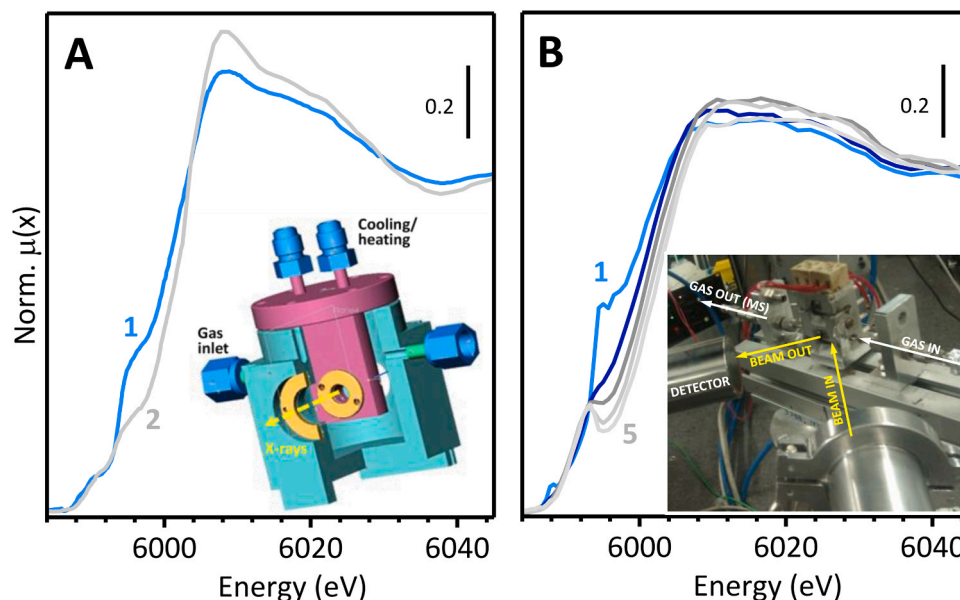

Fig. 2. Part A. Pioneering Cr K-edge XANES spectra of a CO-reduced 4 wt% Cr(II)/SiO₂ catalyst before (spectrum 1) and after (spectrum 2) ethylene polymerization at 100 °C. [64]. The inset shows a scheme of the cell employed for operando XAS experiments in transmission mode at BM08 beamline at ESRF (Grenoble, F). Part B: Operando Cr K-edge XANES spectra collected twenty years later on a CO reduced 1 wt% Cr(II)/SiO₂ catalyst (spectrum 1) and of the same sample during ethylene polymerization at room temperature (from spectrum 2 to 5). [33]. The inset shows a picture of the experimental set-up for operando XAS measurements in fluorescence mode at BM23 beamline at ESRF (Grenoble, F), where the reactor is a quartz capillary.

decouple the influence of the coordination geometry, oxidation state and type of ligands on the electronic properties of a transition metal [70, 71].

For several decades and even before the onset of the *operando* approach, also UV-Vis spectroscopy has played a major role in investigating the properties of the grafted chromium species on both oxidized and CO-reduced Cr(II)/SiO$_2$ catalysts, in the latter case also coupled with the use of probe molecules to understand the accessibility of the Cr (II) sites [32–35,63,72–78]. However, quite curiously, examples where UV-Vis spectroscopy is applied in *operando* conditions, i.e. during ethylene polymerization, are quite rare. One of the first experiments of this type is reported in Fig. 3A [37]. The experiment was performed in transmission mode on a 0.5 mol% Cr(II)/SiO$_2$ monolith (calcined at 500 °C, followed by CO reduction at 350 °C) inside a closed cell equipped with sapphire windows (inset in Fig. 3A). As already discussed above, these are not optimal conditions for catalysts activation (i.e., temperature lower than 600 °C and metallic cell). The spectrum of the catalyst (spectrum 1 in Fig. 3A) is characterized by two peculiar bands at 770 nm (13000 cm^{-1}, $\varepsilon = 2240$ M^{-1} cm^{-1}) and at 1229 nm (8150 cm^{-1}, $\varepsilon = 354$ M^{-1} cm^{-1}), which were ascribed to d-d transitions of low symmetry Cr(II) sites [37]. The catalyst was then exposed to sequential ethylene pulses at 1 atm and 80 °C and UV-Vis spectra were collected at each pulse, following a strategy similar to that employed years before for IR spectroscopy. After interaction with ethylene, the two above-mentioned bands disappear in favour of two resolved but strongly overlapping bands at 676 nm (14800 cm^{-1}, 1240 M^{-1} cm^{-1}) and 463 nm (21600 cm^{-1}, 1570 M^{-1} cm^{-1}), which were assigned to Cr(III) species with a symmetry lower than octahedral [37]. The assignment was corroborated by a complementary EPR experiment, which highlighted the formation of Cr(III) species. The two experimental observations together were considered as a proof that Cr(III) are the active species in ethylene polymerization. However, it is important to notice that in the adopted experimental conditions, only organo-Cr(III) species were formed (an average C/Cr ratio = 1.9 ± 0.2 was estimated by elemental analysis). Even considering that only a fraction of the chromium sites are active, this value does not account for the formation of PE chains. Hence, the UV-Vis spectra reported in Fig. 3A might be of scarce significance for the active species, while they are more probably representative of catalyst deactivation, which is likely to occur in defect of monomer.

On the other hand, Fig. 3B shows the results of a similar UV-Vis experiment performed in diffuse reflectance (DR) mode on a Cr(II)/SiO$_2$ catalyst in the form of powder inside a quartz reactor optimized for reflectance measurements, working in this case in "batch conditions" [33]. Before interaction with ethylene, the catalyst was light blue in colour (inset in Fig. 3B) and its UV-Vis spectrum (spectrum 1 in Fig. 3B) is similar, but not the same, as that reported in Fig. 3A, with the two d-d bands slightly red-shifted at 830 and 1350 nm (ca. 12000 and 7500 cm^{-1}), an intense band at 335 nm (about 30000 cm^{-1}, assigned to O→Cr charge-transfer transition), which was out from the measured range in Fig. 3A. These differences are due to the different thermal history of the two catalysts: calcination at higher temperature (650 vs. 500 °C) is known to favour the formation of more under coordinated Cr (II) sites [80]. Therefore, the energy position of the d-d bands is strongly influenced by the coordination geometry: lower the metal coordination, lower the energy of the transition. Afterwards, as soon as ethylene interacts with the catalyst, the powder turns from light blue to dark blue; correspondingly, in the DR UV-Vis spectrum (spectrum 2 in Fig. 3B), the fingerprints of highly under coordinated Cr(II) sites immediately upward shift. Although the spectral behaviour is similar to that observed in Fig. 3A, the interpretation was sensibly different. In particular, the upward shift of the d-d bands was taken as a straightforward indication that the coordination sphere around the Cr(II) sites is expanded due to π-adsorbed ethylene. Two independent experimental observations were in favour of this interpretation: 1) a very similar DR UV-Vis spectrum was obtained upon exposing the same sample to cyclohexene, a cyclic olefin that can only coordinate to the Cr(II) sites, without polymerizing [23,81]; 2) no evidences for Cr(III) formation were obtained in a complementary *operando* EPR experiment, despite the extremely high sensitivity of the technique towards Cr(III) species [79]. Opposite to the previous case, the occurrence of ethylene polymerization was demonstrated by the appearance of sharp bands in the NIR region of the spectra (Fig. 3B), attributed to the overtones and combinations of the fundamental CH$_2$ vibrational modes. During the polymerization, the powder rapidly becomes white (inset in Fig. 3B), and correspondingly the whole UV-Vis spectrum decreases in intensity (spectra 3 and 4), preventing the detection of the spectroscopic features associated to the active chromium species. This frustrating observation was ascribed to the scattering of visible light by the combination catalyst + polymer [23,33]. As a matter of fact, neither the polymer nor the catalyst are white in colour.

In conclusion, neither XAS nor UV-Vis *operando* spectroscopies, *alone*, are able to provide a definite answer on the oxidation state of the active chromium sites in the Phillips catalyst, but both of them are able to identify the fingerprints of the chromium species involved in ethylene polymerization.
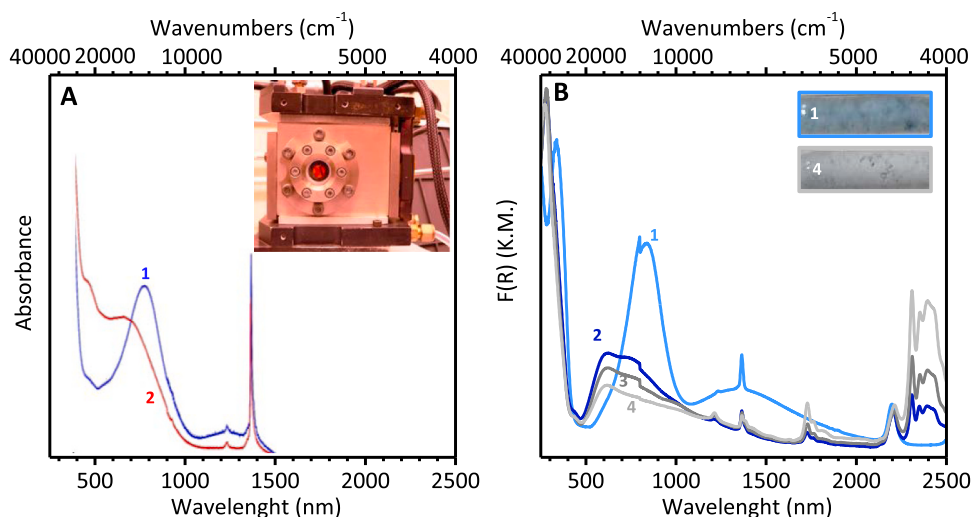

Fig. 3. Part A: UV-Vis spectra collected in transmission mode on a CO-reduced Cr(II)/SiO$_2$ monolith before (spectrum 1) and after (spectrum 2) exposure to sequential ethylene pulses at 80 °C. The inset shows a picture of the cell employed for the measurements [37]. Part B: DR UV-Vis spectra of a CO-reduced Cr(II)/SiO$_2$ sample before (spectrum 1) and after (from spectrum 2 to 4) exposure to an excess of ethylene at room temperature. A picture of the sample before and after ethylene polymerization is shown in the inset. [33,79].

2.2. The induction time during ethylene polymerization on the oxidized Cr(VI)/SiO₂ catalyst

Another question that had triggered the scientific community since the discovery of the Phillips catalyst is what happens in the polymerization reactor during the so called "induction time", that is the time during which the oxidized Cr(VI)/SiO₂ system is reduced by ethylene (at a temperature of 80 – 110 °C) to give reduced chromium intermediates and some oxidation byproducts. The two main subjects of debate have been the type of byproducts and the nature of the reduced chromium sites, in terms of molecular structure, oxidation state, and local geometry. The main experimental difficulty in answering to these questions is the fact that ethylene acts simultaneously as reducing agent and monomer, hence the reduction of the Cr(VI) sites occurs almost simultaneously to the onset of polymerization [28–31,82,83].

For what concerns the ethylene oxidation byproducts, formaldehyde has been long claimed as the most probable one on the basis of chemical intuition [36,84–88]. However, direct experimental observation of formaldehyde was rare. Only in recent times, on the basis of thermogravimetric and calorimetric measurements, Mc Daniel and collaborators hypothesized the possibility that other oxygenated byproducts can be formed (such as ketones, aldehydes, carboxylates or esters) and, even more important, that under commercial polymerization conditions these oxygenates may be retained by the catalyst, remaining in the chromium coordination sphere [82]. The first (and probably unique so far) spectroscopic evidence on the nature and location of the ethylene oxidation byproducts was provided a few years later, by combining *operando* IR, XANES, UV-Vis and EPR spectroscopies [23,33,79,89]. Fig. 4 reproduces the DR UV-Vis and IR results, while discussion of XANES and EPR spectra can be found in the original works.

The sequence of *operando* DR UV-Vis spectra of Cr(VI)/SiO₂ collected at 150 °C in presence of ethylene (Fig. 4A-A'') reveals the existence of two temporal regimes. Initially (spectra 1–10), the spectroscopic fingerprints of the monochromate species (bands at ca. 28000 and 21500 cm⁻¹, assigned to O→Cr(VI) charge-transfer transitions) slowly decrease in intensity, and simultaneously two peculiar d-d bands appear at 16700 and 9500 cm⁻¹ (Fig. 4A''), which were ascribed to 6-fold coordinated Cr(II) sites. PE is formed only at a later stage (spectra 11–18), as revealed by looking to the NIR region (Fig. 4A'). During the polymerization, not only the remaining fraction of Cr(VI) sites is further reduced, but also the two d-d bands characteristic for 6-fold coordinated

Cr(II) intermediates disappear, unambiguously indicating that these sites are rapidly embedded into the growing polymer and hence involved in the polymerization reaction.

As far as the nature of the by-products is concerned, further insights were provided by *operando* IR spectroscopy. A representative sequence of IR spectra collected in conditions analogous to those of Fig. 4A-A' is reported in Fig. 4B-B'. The spectra are reported after subtraction of that collected prior the entrance of ethylene in the reaction cell. At the very beginning of the reaction (spectra 1–3), when PE is not yet formed but chromate species start to be reduced, absorption bands are observed in both the $\nu(CH_x)$ region (Fig. 4B) and in the 1750 – 1300 cm⁻¹ range (Fig. 4B'), which cannot be attributed to PE, but rather to the byproducts of ethylene oxidation in interaction with the reduced Cr(II) sites. In particular, the band at 1585 cm⁻¹ and its shoulder at higher frequency are particularly intense, which unambiguously indicates that they are due to functional groups with high extinction coefficients (such as organic carbonyls, formates, and others). Complementary measurements indicated that the most accredited byproduct is methylformate [23], which originates from disproportion of two formaldehyde molecules at the same Cr(II) site [90]. Depending on the coordination mode, the $\nu(C{=}O)$ band of methylformate can contribute at slightly different position, but always largely red-shifted with respect to the unperturbed molecule (1720 cm⁻¹) due to the strong Lewis acid nature of the reduced chromium sites. On the basis of the literature of methylformate adsorbed on other systems [91,92], the band at 1585 cm⁻¹ is attributed to methylformate ligated to the Cr(II) sites in a bidentate fashion. At longer reaction times (spectra 4–7), simultaneously to the reduction of the remaining Cr(VI) species, ethylene polymerization also takes place, as evidenced by the appearance of intense absorption bands in the $\nu(CH_2)$ and $\delta(CH_2)$ spectral regions (at 2920 and 2850 cm⁻¹ and at 1470 cm⁻¹, respectively). Concurrently, in the 1750 – 1300 cm⁻¹ range, a new band appears around 1650 cm⁻¹, which is attributed to methylformate ligated to the reduced chromium sites through the C=O moiety in a monodentate fashion. The relative intensity between the two bands at 1585 and 1650 cm⁻¹, i.e. the relative fraction between bidentate and monodentate methylformate species, changes with time. In particular, the monodentate species become progressively favoured as soon as the polymer grows (likely because of the increasing steric hindrance of the growing chains). These data demonstrate that the oxygenated by-products remain in the chromium coordination sphere also during ethylene polymerization, and are characterized by a flexible behaviour,
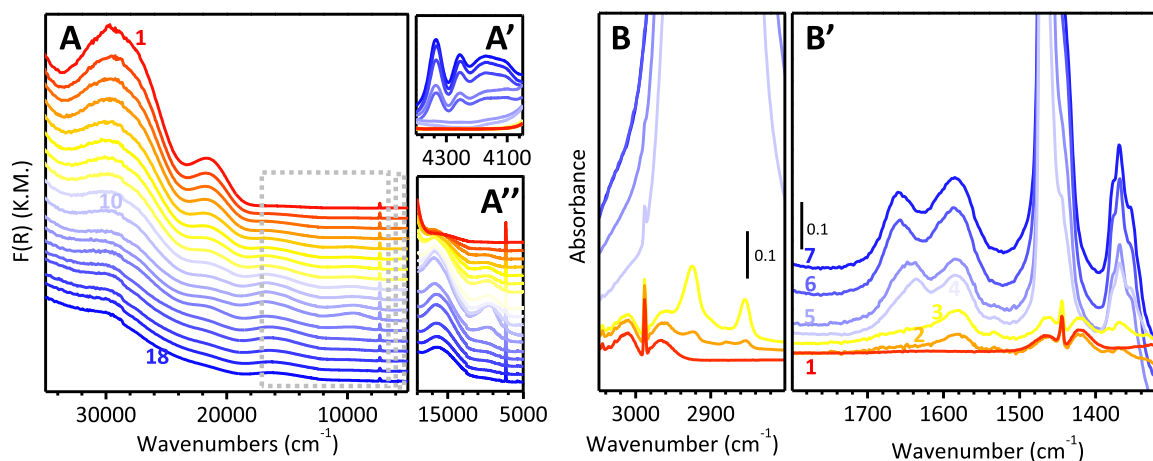

Fig. 4. Part A: Time evolution of the DR UV-Vis spectra of Cr(VI)/SiO₂ in presence of ethylene at 150 °C. From spectrum 1 to 10: induction time; from 11 to 18: polymerization. The inset shows a magnification of the NIR region where appear the vibrational features of PE. Part A': the same as part A, magnified in the region characteristic for the d-d transitions of reduced Cr(II) intermediates. Reproduced from Refs. [23,33]. Part B: Time evolution of the IR spectra of Cr(VI)/SiO₂ in presence of ethylene at 150 °C. The colour code is the same as in part A. The spectra are shown after subtraction of the spectrum of the catalyst prior interaction with ethylene. Part B': the same as part B in the region characteristic of the vibrations of the oxygenated byproducts. Unpublished spectra that reproduced the conditions of Ref. [23].

which is influenced by the presence of the polymer in the surroundings [24].

Interestingly, a few years later similar IR and DR UV-Vis *operando* experiments were performed during photo-activation, i.e. during irradiation with UV−Vis light, demonstrating that Cr(VI)/SiO$_2$ undergoes photo-reduction by ethylene already at room temperature, followed by rapid polymerization [93]. Fig. 5 summarizes the main results. The experiment was performed by using a Newport 500 W Hg(Xe) arc lamp for UV-Vis irradiation. During the IR measurements, the radiation was focused on the sample using an aspherical fibre bundle focusing assembly and a large core liquid light guide, which allowed to collect the IR spectra during continuous UV-Vis irradiation. For the DR UV-Vis measurements, instead, the radiation was not focused, in order to maximize the number of photons reaching the sample, and the measurements were performed sequentially to the irradiation steps.

The DR UV-Vis spectrum of Cr(VI)/SiO$_2$ rapidly changes upon UV-Vis irradiation in the presence of ethylene (Fig. 5A-A''), following a two-step process similar to that discussed above for the thermal reduction by ethylene. After less than 50 s of irradiation (from spectrum 1 to 3), the absorption bands associated to the monochromate species (28000 and 21500 cm^{-1}) decrease in intensity, simultaneously to the appearance of the two bands at ca. 16700 and 9500 cm^{-1} characteristic for 6-fold coordinated Cr(II) species. During this step no ethylene polymerization occurs (Fig. 5A'). Later on (spectra 4–7), ethylene polymerization starts and efficiently proceeds for longer irradiation times (inset in Fig. 5A). However, as soon as the catalyst is embedded into the polymer, the DR UV-Vis spectra decrease in intensity and the fingerprints of the active chromium species disappear, as already discussed above.

Fig. 5B and B' shows the results obtained during a complementary *operando* IR experiment. During the first minute of UV-Vis irradiation, a series of IR absorption bands appear in the $\nu(CH_x)$ stretching region (Fig. 5B) and in the $1750 - 1300$ cm^{-1} range (Fig. 5B'), which are attributed to the byproducts of ethylene oxidation in interaction with the reduced chromium sites. The spectra are much more complex than those collected during the thermal reduction of Cr(VI)/SiO$_2$ by ethylene. Beside methylformate coordinated to the Cr(II) sites in both monodentate (1650 cm^{-1}) and bidentate (1585 cm^{-1}) modes, also ethylene oxide coordinated to partially oxidized Cr(IV)=O species can be detected (the most recognizable band is the one at 3030 cm^{-1}) [94]. Ethylene polymerization starts after ca. 2 min of continuous UV-Vis irradiation and proceeds in the presence of both types of oxidized byproducts. Interestingly, the absorption bands assigned to methylformate keep on

growing also during ethylene polymerization. This indicates that the polymerization rapidly starts at a few highly reducible chromium sites, while other sites are less reducible and start later.

The data summarized in Fig. 5 demonstrate that UV-Vis light efficiently triggers ethylene polymerization on the Cr(VI)/SiO$_2$ catalyst already at room temperature. During the induction time two types of oxidized byproducts have been detected by *operando* IR spectroscopy: methylformate and ethylene oxide, the latter not observed during the thermally induced ethylene polymerization. It was suggested that this is due to the specific photoactivation mechanism for Cr(VI), which involves a single oxygen removal per time passing through the formation of a Cr^V(=O)(O$^-$)* excited state. Once more, the fundamental role of *operando* IR spectroscopy in recognizing the by-products of ethylene oxidation is clear, while *operando* DR UV-Vis spectroscopy is necessary to demonstrate that the oxidation by-products remain in the coordination sphere of the chromium sites during the onset of the polymerization reaction.

3. A step further: *operando* spectroscopies in the presence of Al-alkyl activators

3.1. Genesis of the active sites in MgCl$_2$-based Ziegler-Natta catalysts

3.1.1. Pioneering operando studies on model ZN catalysts

Much later than the first *operando* studies on the Phillips catalysts, we witnessed the appearance in the literature of spectroscopic data collected in the presence of aluminum alkyls. This was not only a consequence of an improvement in the experimental set-ups, but also of an increased awareness of the researchers expert in spectroscopy on the main questions of interest in the field of industrial polymerization catalysis. The possibility to manipulate with confidence Al-alkyls opened the door to the application of *operando* spectroscopies also to other heterogeneous olefin polymerization catalysts, in particular to the Ziegler-Natta ones. Two main experimental strategies have been developed so far for reacting the pre-catalyst powder with the Al-alkyl activator during an *operando* spectroscopic experiment. The first one consists in injecting the desired amount of activator (to attain a specific Al/metal ratio) in an inert flow which passes through the sample. The second method, instead, consists in a classical impregnation of the pre-catalyst powder with the Al-alkyl in a solvent (typically hexane or similar) performed in a glove-box before starting the spectroscopic measurement. Both methods have pros and cons. The former has the
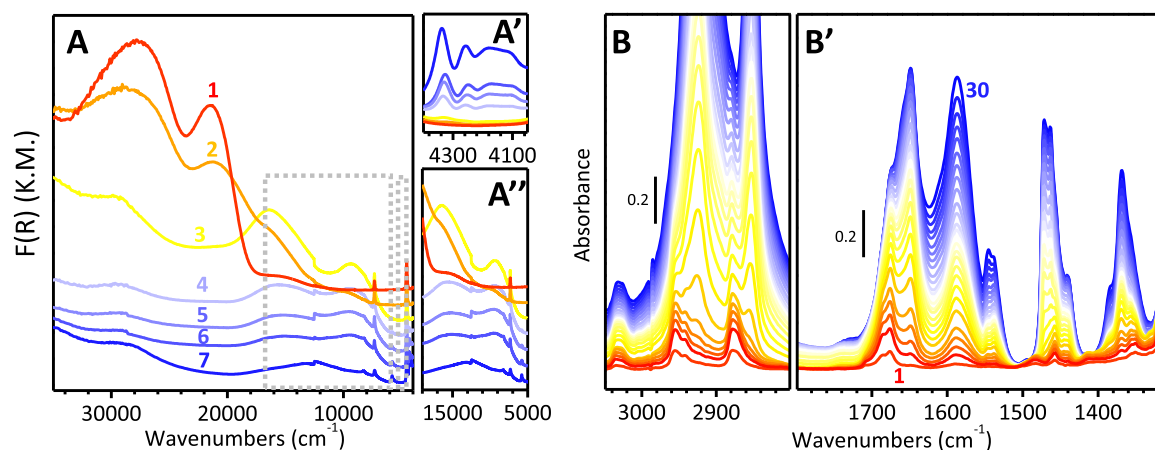

Fig. 5. Part A: Evolution of the DR UV-Vis spectra of Cr(VI)/SiO$_2$ in presence of ethylene at room temperature upon irradiation with UV-Vis light for increasing time. From spectrum 1 to 3: induction time; from spectrum 4 to 7: polymerization. Part A': shows a magnification of the NIR region where appear the vibrational features of PE. Part A'': the same as part A, magnified in the region characteristic for the d-d transitions of reduced Cr(II) intermediates. Part B: Time evolution of the IR spectra of Cr(VI)/SiO$_2$ in presence of ethylene at room temperature upon continuous irradiation with UV-Vis light. The colour code is the same as in part A. The spectra are shown after subtraction of the spectrum of the catalyst prior interaction with ethylene. Part B': the same as part B in the region characteristic of the vibrations of the oxygenated byproducts. Both parts are reproduced from Ref. [93].

advantage that the reaction of the pre-catalyst with the activator occurs directly in the spectroscopic cell, and can be instantaneously monitored by spectroscopy; while in the second case a short time interval passes before the measurement, i.e. the time necessary to transfer the activated catalyst in the reaction cell, extract the cell from the glove-box and position it in the spectrophotometer. On the contrary, when the activation occurs in flow, the control of the Al/metal stoichiometry is more crucial: a fraction of the Al-alkyl may act as scavenger and not as activator and, depending on the experimental set-up, only a fraction of the catalyst powder can effectively react with it, resulting in an altered or not homogenous Al/metal ratio. In this respect, the impregnation method guarantees that all the activator reacts with the pre-catalyst and the persistence of the solvent in the catalyst pores prevents possible fast deactivation, which is usually enhanced in dry conditions.

The first works reporting *operando* measurements on ZN systems date back to the late 2000s, when Thune and co-workers developed a realistic flat model system for MgCl$_2$-based ZN catalysts [95–99], similar to that previously employed to mimic the Phillips catalyst [100–109]. The synthesis method involved the spin-coating of a MgCl$_2$ solution in ethanol (with or without electron donor organic compounds, industrially used as additives to modulate the catalytic performance), either on a flat silicon wafer or directly on the ZnSe crystal used for *operando* ATR-IR measurements (as reported in Fig. 6A), followed by treatment with TiCl$_4$. In the case of ATR-IR measurements, the ATR crystal is successively assembled into a flow cell in inert conditions and finally transferred to the IR spectrophotometer. Then, a solution of triethylaluminum (TEAl) in benzene is saturated with ethylene and flowed through the ATR cell, allowing to monitor in real-time the surface chemistry of the activated catalyst during olefin polymerization. This experimental approach allowed also to perform a morphologic study at the nanometre scale of the catalyst and of the nascent polymer at each stage of catalyst preparation and polymerization, using electron and scanning probe microscopy.

Fig. 6B shows the ATR-IR spectra, in the ν(CH$_2$) region, collected as a function of time during ethylene polymerization on such ZN model catalyst [98]. The observation of the two bands diagnostic for PE at about 2920 and 2850 cm^{-1} (the asymmetric and symmetric ν(CH$_2$) vibrational modes) demonstrates the progressive occurrence of the reaction. Unfortunately, it was not possible to correlate the ATR spectra directly with the polymerization rate, because of intrinsic limitations due to the ATR acquisition mode (e.g. the penetration depth of the evanescent ATR wave depends on the refraction index of the material that is not constant through the whole spectroscopic interval). Nevertheless, this experiment had a pioneering character and demonstrated

the feasibility of *operando* spectroscopic measurements also in the presence of Al-alkyl activators.

A step-by-step approach similar to that discussed above was developed later on also by other groups, including ours, to monitor each step of the synthesis of several MgCl$_2$-based ZN catalysts by combining a series of structural and spectroscopic methods in *operando* conditions [110–117]. Even though in the industrial practice most of the reactions take place all at once within the same reactor, these measurements were fundamental to highlight the occurrence of intermediate transitions that could not have been detected otherwise, but are crucial for the final composition of the catalysts. Some of the results achieved in this field are summarized in the next session.

3.1.2. Attempts to elucidate the nature of the active sites by operando IR spectroscopy

IR spectroscopy has been by far one of the most used experimental technique to investigate the coordination mode of the electron donors in ZN pre-catalysts [24,34,118–126]. In fact, electron donors usually contain functional groups strongly active in IR and particularly sensitive to both the adsorption site and adsorption mode. In contrast, it has been much less exploited to investigate the nature of the active sites generated after reaction of the precatalyst with the Al-alkyl activator. Fig. 7 illustrates some of the difficulties encountered in this field. The investigated system is a model ZN catalyst obtained through a controlled dealcholation of a MgCl$_2$/MeOH precursor, followed by treatment in TiCl$_4$ at 90 °C and subsequent activation by TEAl as co-catalyst at 25 °C [113]. All the steps of the synthesis were performed inside a Harrick Praying Mantis DRIFT accessory equipped with ZnSe windows and connected with a gas flow system, and monitored by *operando* IR spectroscopy. The absence of electron donors greatly simplifies the DRIFT spectrum of the precatalyst (spectrum 1 in Fig. 7A), which shows only a few absorption bands mainly related to a residual fraction of Mg and/or Ti-alkoxide species. Activation by TEAl was accomplished with the "flow" method, injecting a solution of TEAl and hexane in the nitrogen flow. The DRIFT spectrum is immediately saturated by the absorption bands of the hexane solvent (not shown), and only after flushing the system in N$_2$ flow it is possible to appreciate new absorption bands in the ν(CHx) (2950–2800 cm^{-1}) and δ(CH$_x$) (1500–1350 cm^{-1}) regions, which are related to the vibrational modes of the alkyl chains deriving from TEAl (spectrum 2 in Fig. 7A). However, it is not possible to discriminate between alkylated TiCl$_x$R$_y$ species, AlR$_x$Cl$_y$ byproducts, and unreacted AlR$_3$, which likely coexist at the catalyst surface. Even less information on the molecular structure of the active sites can be retrieved by the successive part of the experiment, that is ethylene polymerization at
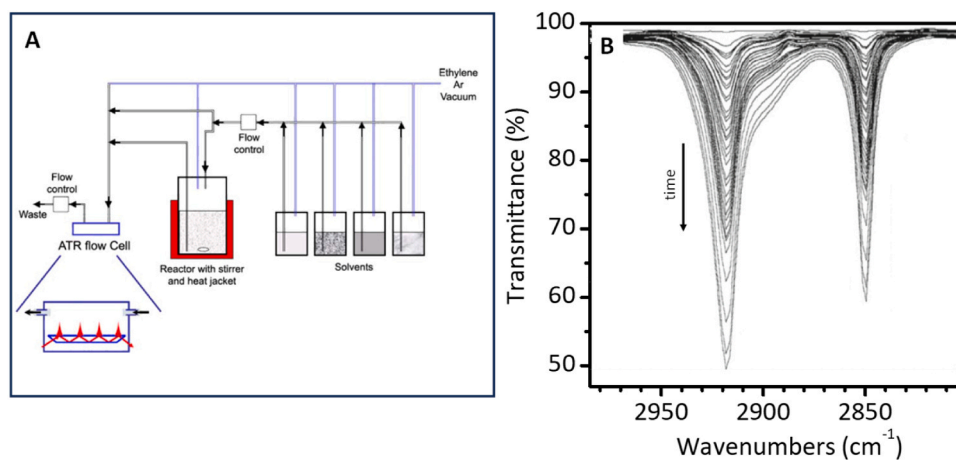

Fig. 6. Part A: Schematic representation of the ATR-IR experimental set-up developed by Thune and co-workers for *operando* investigation of model ZN catalysts, both during the synthesis step, and during ethylene polymerization. Part B: *operando* ATR-IR spectra collected during ethylene polymerization on a model planar MgCl$_2$-based ZN catalyst. Reproduced from Ref. [98].
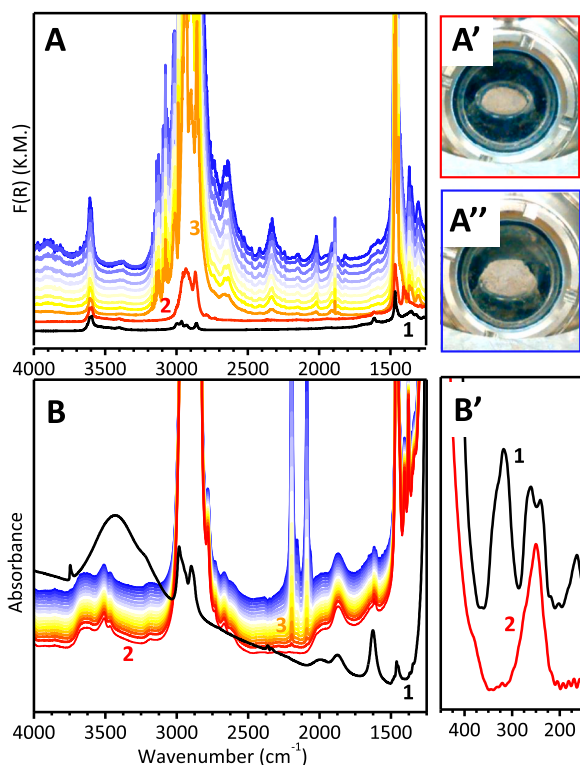
Fig. 7. Part A: *Operando* DRIFT spectra collected during the reaction of a MgCl$_2$/TiCl$_4$ ZN pre-catalyst with TEAl (from spectrum 1 to spectrum 2), and successive ethylene polymerization (N$_2$:C$_2$H$_4$ =75: 25, 20 mL/min, from spectrum 3 onward). The spectra were collected every minute for 10 min. Parts A' and A'': pictures of the catalyst within the Harrick Praying Mantis DRIFT cell before and after ethylene polymerization. [113]. Part B: *Operando* IR spectra collected in transmission mode during the reaction of a silica-supported ZN catalyst obtained from Mg and Ti tetrahydrofuranate precursors during reaction with TEAl (from spectrum 1 to spectrum 2), and successive polymerization of deuterated ethylene (from spectrum 3 onward). Part B': Far-IR spectra of the same silica-supported precatalyst before (spectrum 1) and after reaction with TEAl (spectrum 2), vertically stacked for clarity. [130].

room temperature (20 mL/min, 25% of C$_2$H$_4$ in N$_2$, from spectrum 3 onwards in Fig. 7A). New absorption bands associated to PE grow very rapidly (the already discussed asymmetric and symmetric v(CH$_2$) modes at 2920 and 2850 cm^{-1}, and the δ(CH$_2$) mode at 1470 cm^{-1}), testifying the occurrence of the reaction. Unfortunately, the data cannot be used for quantitatively evaluate the polymerization kinetics. As a matter of fact, during the reaction the catalyst particles enormously increase in size, following the so called "replica effect", according to which the polymer particles replicate the morphology of the catalyst particles, but with a bigger dimension [127–129]. The net effect is that the powder overflows from the sample holder (Fig. 7A' and A''), making the collection of spectra in DRIFT mode no more reliable, because the amount of sample probed by the IR beam is not constant during the experiment.

Similar problems were encountered also during *operando* IR measurements on a silica-supported ZN catalyst based on titanium and magnesium chloride tetrahydrofuranates [130], as shown in Fig. 7B. This type of catalyst was developed in the 1980 s at the Union Carbide Corporation to be used in the UNIPOL process for producing high-density PE [1131–133]. The precatalyst was prepared by reacting together Ti and Mg tetrahydrofuranate precursors in dry tetrahydrofuran (THF), and impregnating with the resulting solution a dehydroxylated SiO$_2$ under a controlled atmosphere. The IR spectra were collected in transmission mode on samples in the form of self-supporting pellets, in both Mid (Fig. 7B) and Far-IR (Fig. 7B') regions, using an

experimental set-up analogous to that described in Fig. 1A. The Mid-IR spectrum of the pre-catalyst (spectrum 1 in Fig. 7B) is dominated by the intense bands due to Si−O vibrational modes of the silica framework (1400 −950 cm^{-1} region) and by their overtone modes (2100 −1550 cm^{-1} region). In the v(OH) region, a broad band is observed at about 3425 cm^{-1}, which indicates the presence of a few OH species H-bonded to a Lewis base (either residual tetrahydrofuranate species or THF). The persistence of residual THF is testified by narrow absorption bands characteristic of THF vibrational modes (v(CH$_2$) at 3050 − 2800 cm^{-1}, δ(CH$_2$) at 1500 − 1300 cm^{-1}, and δ(C-O-C) at 1100 − 600 cm^{-1}). In the Far-IR region the spectrum of the pre-catalyst (spectrum 1 in Fig. 7B') shows several bands, ascribed to v(Mg-Cl) vibrations, similar to those observed in the spectrum of the magnesium tetrahydrofuranate precursor [134].

Addition of the Al-alkyl activator (in heptane as solvent) was performed by "impregnation" method, and caused important changes in the Mid-IR region of the spectrum (spectrum 2 in Fig. 7B). First of all, the spectrum is completely flattened due to the fact that the pellet is wet and hence it does not scatter the IR light anymore. Second, it is dominated by the intense and out-of-scale vibrational modes associated to the alkyl chains of both the activator and the solvent, which prevents understanding the destiny of THF. In contrast, both the solvent and the activator do not contribute in the Far-IR region, where it is possible to observe the disappearance of the vibrational manifestation of the magnesium tetrahydrofuranate precursor, and the appearance of absorption bands characteristic for a highly dispersed and disordered MgCl$_2$ phase (spectrum 2 in Fig. 7B'). This experimental evidence clearly indicates that reaction with the Al-alkyl co-catalyst causes relevant structural rearrangements in the precatalyst, and promotes the formation of small and defective clusters of MgCl$_2$, likely capped by both TiCl$_4$ and THF (or its by-products). Similar conclusions were reached for analogous catalysts not silica-supported [135–137]. Finally, the catalyst performances were monitored by means of *operando* IR spectroscopy. Deuterated ethylene was used, in order to discriminate the PE vibrational modes from the intense absorption bands due to the activator and the solvent. Also in this case, two v(CD$_2$) bands characteristic for PE gradually grow as a function of time (at 2195 and 2089 cm^{-1}), testifying the occurrence of the reaction. The kinetic of ethylene polymerization can be estimated by monitoring the intensity of these two bands as a function of time (vide infra), but no information at a molecular level on the nature of the active Ti sites can be extracted.

The two examples summarized above and several others reported in the literature demonstrate that *operando* IR spectroscopy coupled with a step-by-step synthetic approach is useful to evidence the occurrence of structural transformation in ZN precatalyst upon reaction with the Al-alkyl activators, but alone does not help in elucidating the molecular structure of the active sites, because the spectral regions which might contain diagnostic IR absorption bands are often saturated by the intense absorptions due to the solvent and/or the activator itself. *Operando* IR spectra collected during olefin polymerization can be used to evaluate the catalytic activity of ZN catalysts, but quantitative analysis should be done with caution, depending on the acquisition mode and experimental set-up.

3.1.3. Elucidating the electronic properties of the Ti active species by operando DR UV-Vis and XAS spectroscopies

Opposite to the case of the Phillips catalyst, the mechanism of initiation of olefin polymerization on a ZN catalyst is generally well accepted, i.e. the Cossee-Arlman mechanism [138,139]. The role of the Al-alkyl activator is to reduce and alkylate the starting Ti(IV) sites to Ti(III)-R species, with the simultaneous creation of a coordination vacancy. Hence, there are no controversies on the oxidation state of the active Ti species, even though it is known that unreduced Ti(IV) species, as well as over-reduced Ti(II) ones, may coexist along with Ti(III) species. Nevertheless, the heterogeneous nature and the complexity of the chemical composition in modern ZN catalysts, imply that the Ti(IV) sites

in the precatalysts are generally not all the same, and their relative proportion may also differ from catalyst to catalyst. In particular, both the synthetic method and the type of the electron donors employed play a mayor role in affecting the location of the Ti(IV) sites on the $MgCl_2$ surface, as well as their electronic properties (e.g. electron density at the Ti sites) [140,141]. The nature of the Ti(IV) sites in the pre-catalysts, in turn, affects the properties of the active sites generated by the Al-alkyls in the catalysts.

One of the method potentially useful to monitor the electronic properties of the titanium sites in ZN catalysts is UV-Vis spectroscopy. This is demonstrated in Fig. 8, which summarizes a series of results obtained with DR UV-Vis spectroscopy on different $MgCl_2$-supported ZN catalysts, before and after reaction with the Al-alkyl activator. Three pre-catalysts belong to the class of the so called "mechanically activated" catalysts [122,144–149], and were obtained by ball-milling pristine $MgCl_2$ with $TiCl_4$, either in absence (bm/$TiCl_4$, Fig. 8A), or in presence of electron donors (bm/EB/$TiCl_4$ and bm/DE/$TiCl_4$, Fig. 8B-C, where EB = ethylbenzoate and DE = 1,3-di-ether, specifically 2-isopropyl-2-isopentyl-1,3-dimethoxypropane). The other three pre-catalysts, instead, belong to the "chemically activated" family of catalysts, because they were obtained via chemical routes, starting either from tetrahydrofuranate complexes of Mg and Ti (mgthf/$TiCl_4$, Fig. 8D) [134, 136,137,150,151], or from the decomposition of Mg-ethoxide in the presence of the electron donors and $TiCl_4$ (mge/DBP/$TiCl_4$ and mge/-DE/$TiCl_4$, Fig. 8E-F, where DBP = dibutyl phthalate and DE = 1, 3-di-ether) [152–154]. The spectra of the pre-catalysts (black in Fig. 8) are very different from each other, which means that the electronic properties of the Ti sites are not the same, even though their

formal oxidation state and coordination geometry should be, on average, the same (i.e., +4 and 6-fold coordinated by chlorine ligands). All the spectra are dominated by intense absorption bands in the $25000 – 45000$ cm^{-1} region, which are assigned to charge transfer transitions from the π orbitals centred on the Cl ligands to the 3d orbitals centred on the Ti(IV) sites. Under the approximation of an almost octahedral symmetry, the Ti(3d) orbitals split in energy, causing the appearance of two main sets of bands: bands *A*, at lower energy, are ascribed to Cl(π)→Ti($3d_{t2g}$) transition, while bands *B*, at higher energy, are due to Cl(π)→Ti ($3 d_{eg}$) transition; the difference in energy between the two bands corresponds to the crystal field splitting, Δ_{CF} [143]. It was demonstrated that the energy position of band *A* is particularly sensitive to the effective oxidation state of the Ti(IV) sites: the lower the electron density on the Ti, the lower the energy of the Ti($3d_{t2g}$) molecular orbitals, the lower the position of band *A*, and the higher the splitting energy Δ_{CF} [143]. The details on each sample can be retrieved in the original publications. Herein, we focus the attention on the fact that, in very general terms, the spectra of the pre-catalysts obtained via chemical routes show band *A* at lower energy with respect to those of the samples obtained by ball milling (i.e., a larger Δ_{CF}), which suggests that, on average, the Ti sites are characterized by a lower electron density.

Activation of the precatalysts by Al-alkyl at room temperature causes a drastic change in the DR UV-Vis spectra, and the behaviour is similar, but not the same, for the 6 samples. In all cases, band *A* upward shifts, as expected for a decrease in the Ti oxidation state. The same behaviour is followed by band *B*, which shifts out of the spectral range measurable with accuracy by standard UV-Vis spectrophotometers. The phenomenon is much more relevant for the ball-milled samples, while for the
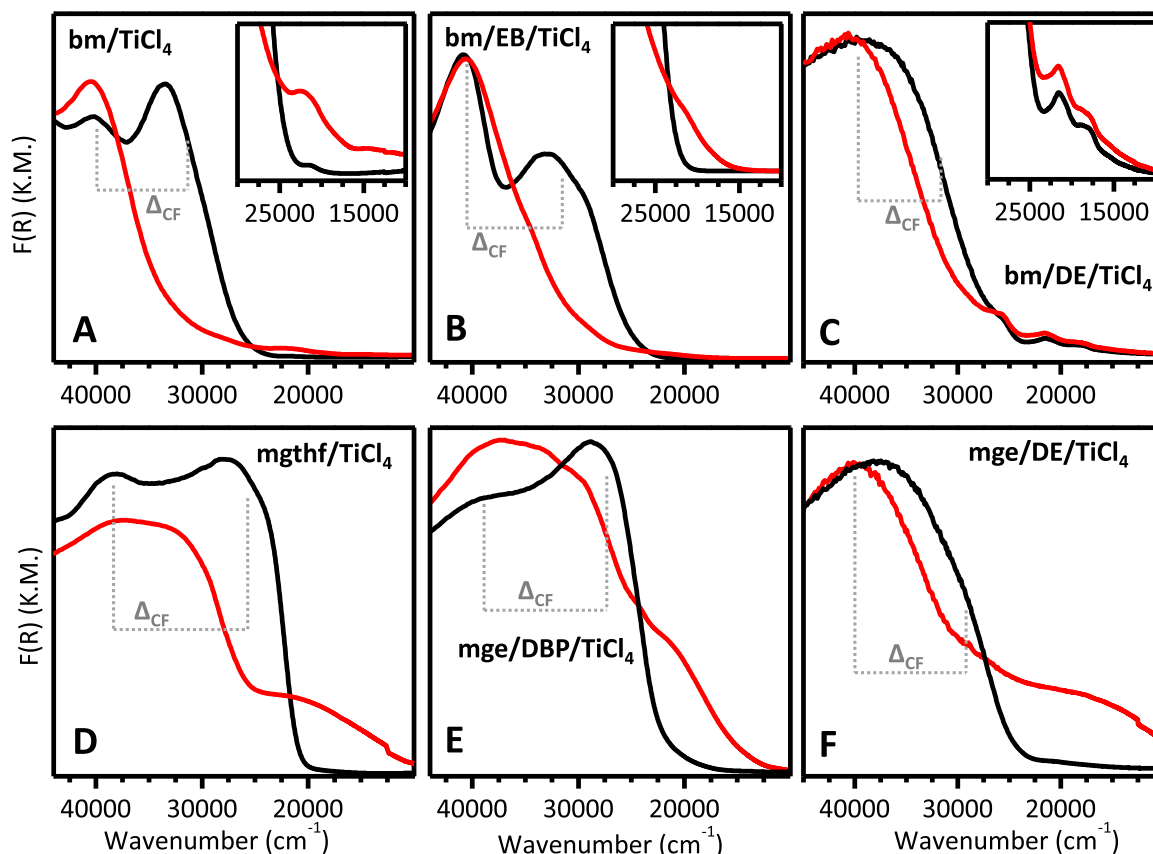

Fig. 8. DR UV-Vis spectra of a series of $MgCl_2$-based ZN catalysts before (black) and after (red) activation by TEAl. Parts A-C refer to pre-catalysts obtained by ball-milling the pristine $MgCl_2$ and $TiCl_4$, either in the absence or in the presence of the electron donors. Insets report a magnification of the low frequency region, containing the fingerprints of isolated Ti(III) sites. Parts D-F refer to pre-catalysts obtained through chemical activation, starting from tetrahydrofuranate precursors of both Mg and Ti, or from decomposition of Mg-ethoxide in the presence of the electron donors and $TiCl_4$. EB = ethylbenzoate; DE = 1,3-diether, DBP = dibutyl phthalate. For each sample, the crystal field splitting Δ_{CF} is also reported. Spectra reproduced from Refs. [130,142,143].

chemically activated ones it does not involve all the Ti(IV) sites, which suggests that the Ti(IV) sites in the latter samples are less reducible [143]. In addition, for the ball-milled samples, a new weak band appear at ca. 22000 cm^{-1} (insets in Fig. 8A-C), which was straightforwardly assigned to d-d transitions of newly formed Ti(III) species. The very weak intensity of these bands suggests that these Ti(III) sites are isolated and retain a 6-fold coordination [24,134,155,156]. In contrast, very intense bands are observed in the same region after activation of the catalysts obtained through chemical routes (Fig. 8D-F). These bands were attributed to inter-site d-d transitions having a partial charge-transfer character, involving two vicinal Ti(III) ions connected through a μ-Cl bridge [24,34,134,157–160], hence taken as an indication for the formation of small TiCl$_3$ clusters. The presence of monomeric Ti(III) sites also in these samples cannot be excluded, however if present their spectroscopic fingerprints would be much weaker and masked by those of the TiCl$_3$ clusters. The lower reducibility of the Ti(IV) sites and the simultaneous observation of TiCl$_3$ clusters in the chemically activated catalysts, are two phenomena in apparent contradiction. They have been explained by considering that, opposite to the case of ball-milled samples, the chemically activated ones contain both micro- and mesopores, which are not necessarily all accessible by TEAl. The Ti (IV) sites located into inaccessible pores are not reduced by TEAl (explaining the lower reducibility of the Ti(IV) sites), while those located inside accessible pores are subjected to severe reducing conditions during drying, and partially mobilized to form TiCl$_3$ clusters [143]. Ethylene polymerization on the activated catalysts generally does not lead to relevant changes in the DR UV-Vis spectra, except for the appearance of the vibrational fingerprints of formed PE in the NIR region and for a small decrease of the overall intensity of the spectra. Hence, once more, DR UV-Vis spectroscopy proves a great utility in unravelling the electronic properties of the pre-catalysts and of the catalysts obtained upon interaction with the Al-alkyl activators, but fails in monitoring the changes occurring at the Ti sites during the polymerization reaction.

One of the last spectroscopic method appeared on the scene of ZN catalysis is Ti L$_{2,3}$-edge NEXAFS spectroscopy. A Ti L$_{2,3}$-edge NEXAFS spectrum originates from Ti(2p) → Ti(3d) electronic transitions and act as a probe of the density of unoccupied valence states. Hence, it is a method very sensitive to the interactions between the metal Ti centre and the ligands, potentially able to discriminate between sites having a similar geometrical environment but yet different electronic properties, and perfectly complementary to UV-Vis spectroscopy [143]. Fig. 9

illustrates the potentials of the method. Fig. 9A (top) shows the *operando* reactor cell for ambient pressure soft X-rays absorption measurements, developed at the APE-HE beamline of the Elettra Sincrotrone Trieste facility [161,162]. The cell, sealed with an ultrathin Si$_3$N$_4$ membrane transparent to the X-ray beam, can be inserted into the ultra-high vacuum chamber necessary to work in the soft X-rays regime. The XAS detection is performed in total electron yield (TEY) mode by probing the drain current from the sample with a picoammeter. A representative picture of the interior of the cell is also shown, with the sample pressed in powder form inside a thin indium plate to guarantee an efficient electric contact (Fig. 9A, bottom).

Fig. 9B shows the Ti L$_{2,3}$-edge NEXAFS spectrum of the bm/EB/TiCl$_4$ catalyst already discussed above, before and after reaction with the Al-alkyl activator. Without entering into many details, the spectrum of the pre-catalyst is characterized by two sets of bands, representing the L$_3$-edge (at lower energy, excitation of an electron from 2p$_{3/2}$ orbitals) and the L$_2$-edge (at higher energy, excitation of an electron from the 2p$_{1/2}$ orbital). Both L$_3$ and L$_2$ edges are further split in two main peaks, due to the splitting of the Ti 3d molecular orbitals. In the approximation of an octahedral symmetry, the two peaks correspond to electronic transitions to the 3d$_{t2g}$ and 3 d$_{eg}$ orbitals, respectively. Hence, the energy difference between these peaks corresponds to the crystal field splitting Δ_{CF}, which is in good agreement with that determined by DR UV-Vis spectroscopy [163]. The spectrum of the pre-catalyst (spectrum 1 in Fig. 9B) was well reproduced by a simplified model containing a 6-fold-coordinated Ti(IV) species on the MgCl$_2$(110) surface (Ti(IV)Cl$_6$ in Fig. 9C and D) [143, 164]. After reacting with TEAl, the Ti L$_{2,3}$-edge spectrum drastically changes (spectrum 2 in Fig. 9B). In particular, new peaks appear at lower energy with respect to those characterizing the spectrum of the pre-catalyst, which were interpreted as due to the reduction of a fraction of the Ti(IV) into Ti(III) sites (just a fraction, since the preexisting signals of Ti(IV) species are still visible, despite less intense). The new features are well reproduced by two models with penta-coordinated Ti(III) species, either surrounded by five chlorine ligands (Ti(III)Cl$_5$ in Fig. 9C and D), or by four chlorine and one alkyl group (Ti(III)Cl$_4$R in Fig. 9C and D), the latter species having all the necessary prerequisites to act as competent site in ethylene polymerization [143].

Finally, ethylene polymerization was carried out by sending ethylene pulses on the catalyst and collecting a spectrum after each pulse, resulting in the sequence reported in Fig. 9B (from spectrum 3 to 6). No new bands are observed in the spectra, as expected, since the electronic features of the active Ti(III)Cl$_4$R sites should be very similar to those of
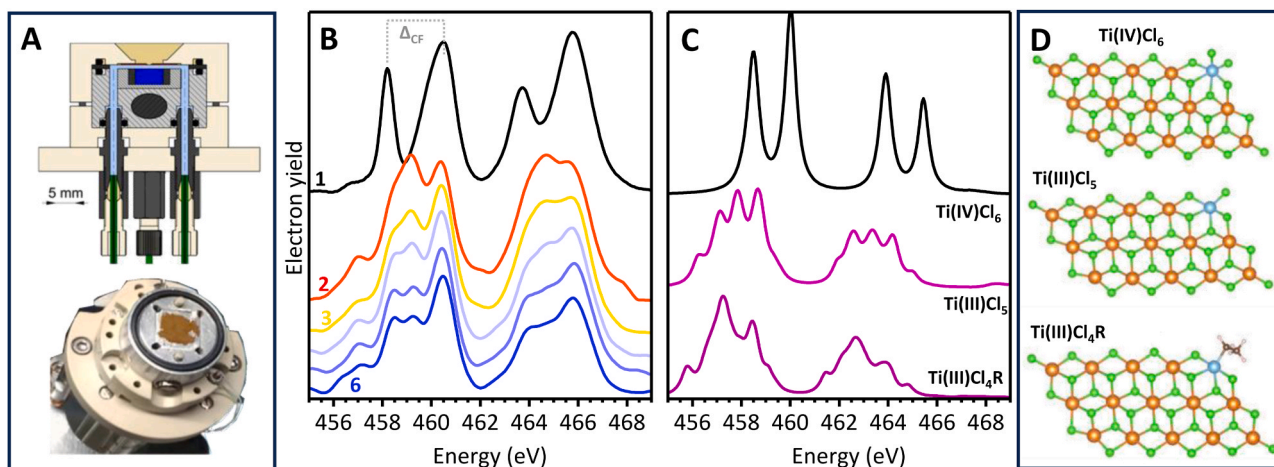

Fig. 9. Part A: scheme of the *operando* reactor cell for ambient pressure soft X-rays absorption measurements, developed at the APE-HE beamline of the Elettra Sincrotrone Trieste facility (top, from Ref. [161]) and picture of a ZN catalyst inserted into the cell prior the measurement (bottom). Part B: Ti L$_{2,3}$-edge NEXAFS spectrum of a ZN catalyst obtained through ball-milling of pristine MgCl$_2$ with TiCl$_4$ in the presence of ethylbenzoate as electron donor before (spectrum 1) and after reaction with TEAl (spectrum 2). The successive spectra (from 3 to 6) have been collected during ethylene polymerization. Part C: Simulated Ti L$_{2,3}$-edge NEXAFS spectra for the simple models reported in Part D. Spectra and pictures reproduced from Ref. [143].

the Ti(III) species carrying the polymer chain. Nevertheless, the total intensity of the NEXAFS spectra decreases along with the sequence, because the insulating polymer formed at the surface of the catalyst particles attenuates the photoelectrons escaping from the absorbing Ti atoms. It is evident that the bands associated with the Ti(III) species decrease faster than the others. Hence, these bands were assigned to the sites involved in the polymerization reaction.

The same experimental approach was also applied to investigate a SiO_2-supported ZN catalyst with a much more complex chemical formulation [165,166]. Interestingly, in that case, the Ti $L_{2,3}$-edge NEXAFS spectrum of the pre-catalyst after reaction with TEAl was not differing too much from that of the pre-catalyst itself, because it was dominated by the fingerprints of a preexisting $TiCl_3$ phase. However, during ethylene polymerization the spectrum completely changes its shape, up to become very similar to that discussed above for activated bm/EB/$TiCl_4$ sample, i.e. with the fingerprints of partially alkylated Ti (III) species. This behaviour was interpreted taking into account that detection by TEY is extremely surface sensitive, hence a fraction of Ti (III) sites in the pre-catalyst might escape detection, because not sufficiently exposed at the surface. During the polymerization, the catalyst particles undergo fragmentation, allowing them to gradually emerge at the surface and thus being detected by TEY-NEXAFS.

3.2. Al-alkyls as modifying agents for Cr(VI)/SiO₂ Phillips catalyst

As discussed above, the Cr/SiO_2 Phillips catalyst does not need to be activated by Al-alkyls co-catalysts for developing activity in ethylene polymerization. However, metal-alkyls are commonly used in the industrial practice to tailor the performances of the catalyst and the properties of the obtained polymers [30,83,167]. Among the main effects, treatment of Cr(VI)/SiO_2 with small amounts of metal-alkyl co-catalyst allows to reduce and alkylate a fraction of the chromium sites, thus contributing to shorten the induction time and to increase the catalyst activity. Moreover, treatment with metal-alkyls modifies the active sites distribution. This in turn affects the properties of the obtained polymer, broadening the molecular weight distribution and increasing the degree of short-branching. The latter properties is attributed to an *in situ* branching mechanism, according to which a fraction of "modified" chromium sites would oligomerize ethylene to α-olefins, which are successively entangled in the polymer chains growing at the remaining chromium sites.

The effects of metal-alkyls on the chromium sites at a molecular level has been the object of investigation in recent times [87,167–176]. Among the first *operando* spectroscopic studies in the field we mention those by Weckhuysen and co-workers [167,173,174], who systematically investigated the structure-performance relationship of several Cr (VI)/SiO_2 catalysts modified by TEAl by means of *operando* IR and DR UV-Vis spectroscopies. Fig. 10A schematically shows the experimental set-up adopted for DR UV-Vis measurements, which includes a gas manifold for sending different gases, a septum for injecting the co-catalyst in the gas flow, a mass spectrometer and a gas sampling bag for GC analysis of the gas phase, and finally a quartz reactor containing the sample, which is interfaced with the UV-Vis spectrophotometer [174]. The experimental set-up adopted for analogous IR measurements was the same, except for the reaction cell, that was a commercial Praying Mantis interfaced with an IR spectrophotometer [173]. Fig. 10B shows the sequence of DR UV-Vis spectra collected during the pre-reaction of the Cr(VI)/SiO_2 catalyst with TEAl (from spectrum 1 to 10). The absorption bands associated to monochromate species slightly decrease in intensity, and at the same time two bands appear around 16000 and 10000 cm^{-1}, which were generically assigned to 6-fold coordinated Cr(III) and Cr(II) species. However, the changes in the spectra are not substantial, and this suggests that the fraction of chromium sites modified by TEAl (i.e. reduced and alkylated) is quite small. Fig. 10C shows the spectra collected during the successive ethylene polymerization step on the TEAl-modified catalyst. During the reaction (from
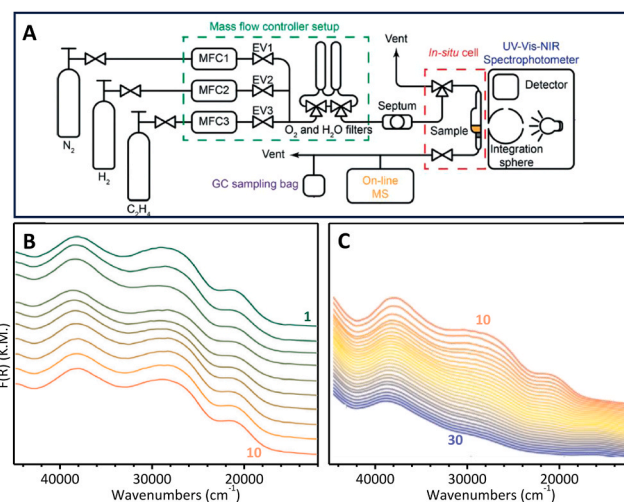

Fig. 10. Part A: Scheme of the experimental set-up adopted by Weckhuysen and co-workers for *operando* UV-Vis measurements on Cr(VI)/SiO_2 during modification by Al-alkyls and successive ethylene polymerization. Part B: sequence of DR UV-Vis spectra collected during reaction of a Cr(VI)/SiO_2 sample with TEAl at 100 °C (from spectrum 1 to 10). Part C: DR UV-Vis spectra collected during the successive ethylene polymerization on the TEAl-modified Cr(VI)/SiO_2 catalyst (from spectrum 10 to 30). Reproduced from Ref. [174].

spectrum 10 to 30), the intensity of the bands associated with monochromate species is drastically reduced at the expenses of the bands associated to the reduced chromium species. Comparison with an analogous experiment performed at the same Cr(VI)/SiO_2 catalyst not modified by TEAl demonstrates that reduction of Cr(VI) during ethylene polymerization is much faster on the TEAl modified catalyst [174].

A similar spectral evolution and similar conclusions were reported also by us in a successive work, were however we have been able to better define the structure of the TEAl-modified chromium sites, by complementing the *operando* approach with the use of molecular probes [171,172]. We confirmed that, in the adopted experimental conditions (Al:Cr=2:1), only 50% of the Cr(VI) were reduced by TEAl, and we identified the reduced species as comprising: 1) 6-fold coordinated Cr (III) sites, not involved in the polymerization reaction; 2) Cr(IV) bisalkylated sites, which are the active sites in the polymerization of ethylene, explaining the faster initiation rate; and 3) two types of mono-grafted Cr(II) sites, having a Lewis acid character, which are responsible for the *in situ* branching and for the broadening of the molecular weight distribution of the obtained polymer.

4. Evaluating the olefin polymerization kinetics by *operando* IR spectroscopy

4.1. Comparing the activity of two or more catalysts in the same experimental conditions

As discussed in the previous sections, *operando* IR spectroscopy has the potential to detect the polymer formation in real time, through the appearance in the IR spectra of absorption bands diagnostic for CH_2 (and CH_3) vibrations. Monitoring the intensity of these bands as a function of time may allow to evaluate the kinetics of ethylene polymerisation, if not strictly quantitatively, at least in a comparative way when working with similar catalysts and the same experimental set-up. Two types of experimental procedures can be found in the literature, where the olefin polymerization is performed either in flow conditions or in batch conditions. In the first case, the monomer is continuously furnished in excess, and the catalyst surface is saturated by it. For this reason the polymerization rate can be considered as independent from the ethylene concentration, and dependent only on the concentration of the active

sites. In the second case, instead, the pressure of the monomer gradually decays as long as the polymerization proceeds. This is the most common way to evaluate the reaction order, and usually in these cases the concentration of the active sites is considered constant throughout the whole experiment, so that the reaction rate depends only on the monomer concentration.

None of these two approaches actually corresponds to the real conditions adopted during industrial gas-phase olefin polymerization. In both cases, the ethylene concentration is much lower than that found in an industrial reactor. Moreover, as anticipated in the introduction, the reactors employed during the spectroscopic measurements do not allow the removal of the heat generated during the olefin polymerization. Hence, over-heating phenomena can take place, and the polymer may melt at the surface of the catalyst particles, preventing further diffusion of the monomer before the occurrence of particle fragmentation. Nevertheless, the polymerization conditions achieved during a spectroscopic experiment are usually considered comparable at least to those employed during the pre-polymerization step in an industrial reactor.

In this respect, a few warnings should be taken in mind. First, when dealing with catalysts activated by Al-alkyls co-catalysts, the use of deuterated ethylene is recommended, to get rid of the intense absorptions in the $\nu(CH_x)$ and $\delta(CH_x)$ regions due to both the co-catalyst and the solvent. Second, comparison between two or more systems should be done at constant catalyst amount. This is not trivial when working with thin pellets for IR measurements. For SiO_2-supported catalysts, normalization to the catalyst amount can be done "spectroscopically", using the absorption bands ascribed to silica as internal reference. Otherwise, quantitative measurements would require evaluation of the sample weight before the spectroscopic experiment.

A nice example of the potentials of the method is reported in Fig. 11, which shows the results of ethylene polymerization at room temperature on a "standard" CO-reduced Cr(II)/SiO_2 catalyst and on the same system modified with a thermal treatment in N_2O, where the Cr(II) sites are selectively converted into grafted chromyl (Cr=O) species [177]. The two experiments were performed with the same experimental set-up shown in Fig. 1A, recording the ethylene pressure, P(C_2H_4), while

simultaneously collecting IR absorption spectra at a 1 s time resolution. Fig. 11A and A' show the IR spectra collected on the two catalysts during the first 2 min of reaction in the $\delta(CH_x)$ region: it is immediately evident that the modified catalyst is by far more active (i.e., IR bands grow faster) than the standard one, and also that the formed PE is the same in the two cases (i.e., same IR bands). By plotting the intensity of the IR band at about 1470 cm^{-1} versus time (Fig. 11B), an almost linear dependence was found in both cases. The modified catalyst shows a very short induction period, which is the time necessary for ethylene to reduce the chromyl species. Comparing the slope of the linear parts of these curves it is possible to obtain information on the relative rate of polymerization, which is approximately twenty times greater in the case of the modified catalyst. The same result is obtained by plotting the P(C_2H_4) versus time (Fig. 11C): a linear trend is observed in both cases, and the pressure decay is almost twenty times faster on the modified catalyst than on the standard one. It is important to notice that the data reported in Fig. 11 refer to the first two minutes of reaction. For longer polymerization times, kinetics data start to be no more reliable. In fact, over heating of the sample causes a partial melt of the polymer around the catalyst particles, with consequent diffusion limitations for the incoming monomer.

4.2. An alternative approach: the use of insertion probes to evaluate the inherent insertion ability of the active sites

The method illustrated above allows to evaluate the activity of two or more catalysts in a comparative way, but cannot give information whether the higher catalytic activity of a certain catalyst is due to a larger amount of active sites, or to an inherent greater ability of the same number of active sites in chain propagation, or a combination of the two. The problem of evaluating the fraction of sites really active in olefin polymerization remains one of the greatest challenges in the field. Very recently, we have started to develop a new experimental approach that can potentially offer an answer to this problem. The strategy is an upgraded version of the active sites tagging technique, which has been used since the discovery of ZN catalysis for active-sites counting [178–186]. It consists in coupling *operando* IR spectroscopy with the use of "insertion probes", which are small molecules able not only to coordinate to the active sites, but also to insert into the metal-alkyl bond, thus mimicking what the monomer does, but without incurring into the diffusion limitations eventually imposed by the presence of the polymer. In short, the method consists in contacting the catalyst with a certain amount of the selected probe. At first, the probe molecule will coordinate to the active sites, showing distinct spectroscopic features depending on the electronic and steric properties of the site. Hence, monitoring the position and the intensity of the corresponding absorption bands it may be possible to differentiate several active sites and also to quantify them. After coordination, the molecular probe will insert into the metal-alkyl bond: monitoring the time evolution of the absorption bands associated to the inserted probe it is possible to extract information on the insertion kinetics [166,187,188].

So far, this approach has been validated for two structurally analogous SiO_2-supported hafnocene and zirconocene catalysts (SiO_2/MAO/Zr and SiO_2/MAO/Hf, respectively, where MAO = methyl alumoxane is the activator) [188]. Despite the structural similarity of the two metallocene precursors, and the same synthetic protocol, SiO_2/MAO/Zr was found to be 40 times more active than SiO_2/MAO/Hf in gas-phase ethylene polymerization. The lower activity of the hafnocene-based catalysts is well-documented in the literature, and attributed to an inherently lower chain propagation rate, which is a consequence of a stronger metal-carbon bond [189–194]. However, it was also demonstrated that in presence of commercial MAO (which unavoidably contains free trimethylaluminum, TMA) rather stable hetero-dinuclear compounds are formed with hafnocene complexes, which are not active in ethylene polymerization [195,196]. Since the two SiO_2/MAO/Zr and SiO_2/MAO/Hf catalysts represented two extremes in terms of activity,
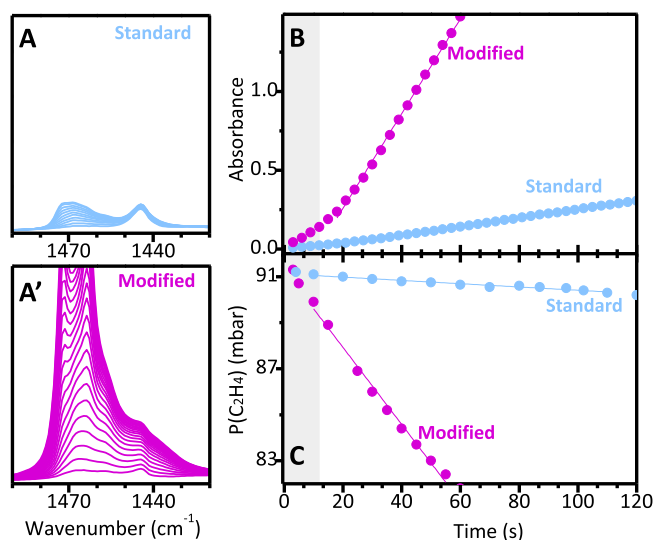

Fig. 11. Part A: Operando IR spectra, in the $\delta(CH_x)$ region, collected during ethylene polymerization at room temperature on a "standard" CO-reduced Cr(II)/SiO_2 catalyst. Part A': the same as part A for the same catalyst previously modified by a thermal treatment in N_2O. Part B: intensity of the IR band at about 1470 cm^{-1} (indicative of the polymer growth) versus time. Part C: evolution of the ethylene pressure as a function of time during the same experiments. The relative polymerization rate is obtained by comparing the slope of the best linear fits, performed on all the time interval but the first 10 min (grey region in parts B and C). Reproduced from Ref. [177].

they were also ideal candidates for testing our approach. Among the possible molecular probes, we focused our attention on deuterated acetonitrile, which is capable to coordinate to transition metal sites with a Lewis acid character and also to insert into transition metal-alkyl bonds to give aza-alkenylidene species. Deuterated acetonitrile (CD_3CN) was used to overcome Fermi resonance effects, which would result in splitting of the absorption bands.

Fig. 12A and B show the sequence of *operando* IR spectra collected as a function of time during interaction of CD_3CN with the two catalysts. An analogous experiment was performed also on SiO_2/MAO as a reference [188]. The initial spectra of the two catalysts (spectra 1) are very similar to each other and are dominated by the vibrational modes of silica and by a few, narrow, bands ascribed to MAO and/or products of the reaction between MAO and SiO_2. As soon as CD_3CN is inserted into the reaction cell (from spectrum 2 onwards), intense absorption bands appear in the 2400 – 2100 cm^{-1} range, which are due to both physisorbed and chemisorbed CD_3CN. Without entering into the details of the spectra, we focus the attention on three bands only. Band *T* (*total*) at 2108 cm^{-1}, which is due to the $\nu(CD_3)$ mode, is insensitive to the adsorption sites [197], and it has been used as an internal standard to quantify the total amount of CD_3CN on each sample. Band *C* (*coordinated*), centred at ca. 2320 cm^{-1}, is ascribed to CD_3CN chemisorbed to the Lewis acid sites (LAS) in the system [171,172], which are both the Al cations belonging to MAO/TMA (dominant species), as well as the zirconocene/hafnocene cations generated after the reaction of the metallocene precursors with MAO. The band rapidly saturates, hence the total amount of accessible LAS has been monitored by tracking the intensity of the band at 2300 cm^{-1}. Finally, bands *I* (*inserted*) at 1684 and 1690 cm^{-1} for $SiO_2/MAO/Zr$ and $SiO_2/MAO/Hf$, respectively, are attributed to the $\nu(C\equiv N)$ vibrations of the aza-alkenylidene species which are formed after the insertion of CD_3CN into the Zr-CH_3 and Hf-CH_3 bonds [198–200].

A couple of systematic experiments were performed by varying the amount of CD_3CN in the reaction cell and monitoring the temporal evolution of the three aforementioned bands [188]. The behaviour is reported in Fig. 12C and D for $SiO_2/MAO/Zr$ and $SiO_2/MAO/Hf$, respectively. It is evident that, for both catalysts, bands *T* and *C* reach immediately their maximum intensity, revealing that coordination of CD_3CN is not limited by diffusion or mass-transfer phenomena. The amount of coordinated CD_3CN (intensity of band *C*) depends on the total amount of CD_3CN in the cell (intensity of band *T*): the higher *T*, the higher the fraction of the sites able to coordinate CD_3CN. Moreover, $SiO_2/MAO/Zr$ coordinates much more CD_3CN than $SiO_2/MAO/Hf$. This indicates that the amount of active sites in $SiO_2/MAO/Hf$ is lower than in $SiO_2/MAO/Zr$, which is a direct consequence of the formation of inaccessible hetero-dinuclear compounds between TMA and hafnocene complexes. Finally, band *I* slowly increases with time, which indicates that insertion into the metal-alkyl bond is an activated process. For both catalysts, the insertion rate (intensity of band *I* over time) is proportional to the amount of coordinated CD_3CN (intensity of band *C*). However, by normalizing the intensity of band *I* to that of band *C*, it is possible to determine the inherent insertion ability of the two catalysts, which is almost the double for $SiO_2/MAO/Zr$, in very well agreement with previous findings in the literature.

In order to demonstrate that the results obtained in the presence of CD_3CN are relevant for olefin polymerization reactions, polymerization of 1-hexene over $SiO_2/MAO/Zr$ and $SiO_2/MAO/Hf$ catalysts was also followed by means of time-resolved *operando* IR spectroscopy. The results are shown in Fig. 13A and B in the most interesting spectral region. The band at 1640 cm^{-1} (*M,* monomer), ascribed to the $\nu(C=C)$ vibrational mode of 1-hexene, was used to evaluate the monomer concentration on the sample, while the band at 1378 cm^{-1} (band *P*, polymer), ascribed to the $\delta(CH_3)$ vibrational mode, was taken as an indication of the amount of growing polymer. The intensity of bands *M* and *P* was

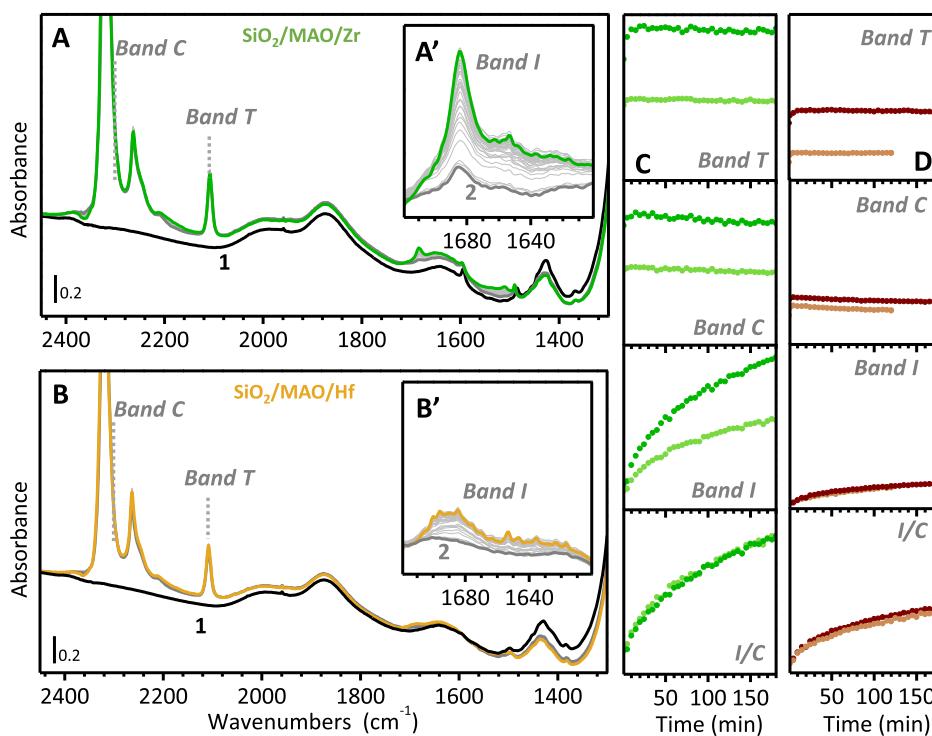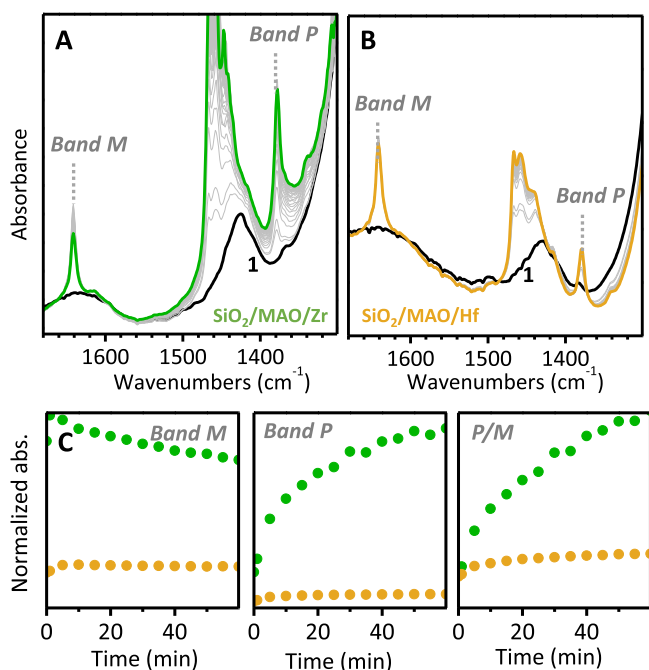**Fig. 12.** Part A: *operando* IR spectra collected on a $SiO_2/MAO/Zr$ catalyst before (spectrum 1) and after (from spectrum 2 onward) coordination of CD_3CN to the LAS sites in the system and its successive insertion into the Zr-CH_3 bond. Bands *T*, *C* and *I* refer to the total, coordinated and inserted CD_3CN, respectively. The inset A' shows a magnification of band *I*. Parts B and B': the same as parts A and A' for a structurally analogous $SiO_2/MAO/Hf$ catalyst. Part C: Evolution of the intensity of bands *T*, *C* and *I* over time and ratio between the intensity of bands *I* and *C*, for the $SiO_2/MAO/Zr$ catalyst. Part D: the same as part C for the $SiO_2/MAO/Hf$ catalyst. Reproduced from Ref. [188].

Fig. 13. Part A: *operando* IR spectra collected on a SiO₂/MAO/Zr catalyst before (spectrum 1) and after (from spectrum 2 onward) homo-polymerization of 1-hexene. Bands *M* and *P* refer to coordinated monomer and growing polymer, respectively. Part B: the same as part A for a structurally analogous SiO₂/MAO/Hf catalyst. Part C: Evolution of the intensity of bands *M* and *P*, and their ratio, for both catalysts. Unpublished data.

followed as a function of time (Fig. 13C). It is evident that the intensity of band *M* is much higher for SiO₂/MAO/Zr than for SiO₂/MAO/Hf, indicating that 1-hexene has more difficulties to penetrate between the ion-pairs in SiO₂/MAO/Hf catalysts, in perfect agreement with previous results obtained in presence of CD₃CN. For SiO₂/MAO/Zr catalyst the decrease in intensity of band *M* over time is more pronounced then for SiO₂/MAO/Hf, and consequently band *P* grows faster, indicating a faster polymerization rate. Fig. 13C reports the ratio between bands *P* and *M*, clearly displaying that the inherent insertion rate of the two catalysts is different, being SiO₂/MAO/Zr inherently faster than SiO₂/MAO/Hf, in well agreement with the data obtained with CD₃CN.

The results summarized in Fig. 12 and Fig. 13 demonstrate the high potential of *operando* IR spectroscopy coupled with the use of insertion molecular probes in investigating the relative fraction of accessible sites and their inherent ability in inserting the monomer into the metal-alkyl bond. This approach is still under development. It works well for heterogenized metallocene-based catalysts, where the active sites are relatively homogeneous. Some preliminary data have been already collected also in the field of ZN catalysts, but further validation is still needed.

5. Unravelling synergistic effects by *operando* IR spectroscopy

5.1. In situ branching in chromium-based catalysts

In Section 3.2 we have already introduced the concept of the *in situ* branching, which is a way to obtain Linear Low Density PE (LLDPE) from neat ethylene polymerization, without the addition of α-olefins as co-monomers in the feed. This process is particularly advantageous with respect to the traditional co-polymerization of ethylene and α-olefins, because ethylene is much cheaper and more widely available than the co-monomers and because the incorporation efficiency of the α-olefins in the growing polymer is much higher when they are produced *in situ* instead of being added externally [30,60]. The *in situ* branching

mechanism typically occurs on the Phillips catalyst when it is opportunely modified with some activators, as already discussed in Section 3.2: in these cases, α-olefins are produced through ethylene oligomerization by a fraction of chromium sites modified by the co-catalyst (hereafter labelled as Cr$_{oligom}$), and successively entangled into the polymer chains growing on the remaining, unmodified, sites (hereafter labelled as Cr$_{polym}$). In the last decades, quite a lot of efforts has been devoted to elucidate the molecular structure of the chromium sites modified by several co-catalysts, by means of a multi-technique approach comprising several spectroscopic methods, as well as the analysis of the obtained polymer [87,167–176,201,202]. While IR spectroscopy is rarely informative on the structure of the modified sites, *operando* IR spectroscopic experiments are extremely useful to unravel the occurrence of *in situ* branching, and the cooperation between different types of active sites.

Among all the possible co-catalysts, hydrosilanes remain the most effective ones for inducing *in situ* branching on the Phillips catalyst. Fig. 14 shows the time-resolved IR spectra collected during the first 8 min of ethylene polymerization on a "standard" CO-reduced Cr(II)/SiO₂ catalyst (parts A-D), and on the same catalyst after modification with SiH₄ (parts E-H) [202]. The spectra are shown after subtracting that collected before the entrance of ethylene in the reactor and normalized to the optical thickness of the pellet. By comparing the two sequences of spectra, it is immediately evident that ethylene polymerization is much faster on the SiH₄-modified catalyst (i.e., the IR absorption bands associated with the polymer grow much faster), but also that the obtained polymer is different in the two cases (i.e., the number and position of the bands is different). While on the standard catalyst the IR spectra are characterized by the usual bands ascribed to the CH₂ vibrational modes of long and linear PE chains ($\nu(CH_2)$ at 2920 and 2850 cm⁻¹, $\delta(CH_2)$ at 1472 cm⁻¹, Fig. 14B and D), on the SiH₄-modified catalyst additional bands assigned to CH₃ groups are also clearly observed in both the stretching and bending regions ($\nu(CH_3)$ at 2970 and 2880 cm⁻¹, $\delta(CH_3)$ at 1380 cm⁻¹, Fig. 14F and H). Fig. 14 shows also the spectral behaviour in the $\nu(OH)$ (parts A and E) and $\nu(C=C)$ regions (parts C and G). During ethylene polymerization on the standard catalyst, a new $\nu(OH)$ band gradually grows at 3695 cm⁻¹, at the expenses of the band ascribed to isolated silanols (3747 cm⁻¹): this behaviour indicates that a fraction of surface silanol groups interact with the polyethylene chains via H-bonding. No bands are observed in the spectral region where $\nu(C=C)$ modes should contribute (part C). On the SiH₄-modified catalyst, instead, two additional bands are observed at about 1638 cm⁻¹ and at 3570 cm⁻¹. These bands are ascribed to the $\nu(C=C)$ vibrational mode of 1-hexene and to surface OH groups H-bonded to 1-hexene, respectively. The weak intensity of these bands is attributed to the very fast incorporation of the 1-hexene formed at the Cr$_{oligom}$ sites into the polymer chains growing at the Cr$_{polym}$ sites.

Another interesting case study is constituted by the organo-chromium Cr[CH(SiMe3)₂]₃/SiO₂ catalyst, prepared by grafting the Cr [CH(SiMe3)₂]₃ precursor onto a highly dehydroxylated silica, which is highly effective in ethylene polymerization even at room temperature and without any pre-activation treatment [204,205]. It has been demonstrated that this catalyst contains two types of Cr(III) sites, which either oligomerize ethylene affording α-olefins (Cr$_{oligom}$) or homo- and copolymerize it to give a branched PE (Cr$_{polym}$). These two types of sites cooperate in tandem, as already demonstrated for the silane-modified Phillips catalyst. Moreover, the relative amounts of the two types of sites are a function of both the chromium loading and the silica activation treatment. In particular, by keeping constant the calcination temperature, an increase in the chromium loading leads to an overall decrease in the activity per chromium site, and also to a drastic decrease in the polymer density. For catalysts on SiO₂ preactivated at 600 °C, a slight increase of the chromium content from 0.1 to 0.4 wt% causes a decrease of the polymer density from 0.9590 to 0.9065 g/cm³, which indicates that the relative amount of the Cr$_{oligom}$ sites with respect to the Cr$_{polym}$ ones increases with the chromium loading [204,205]. This is
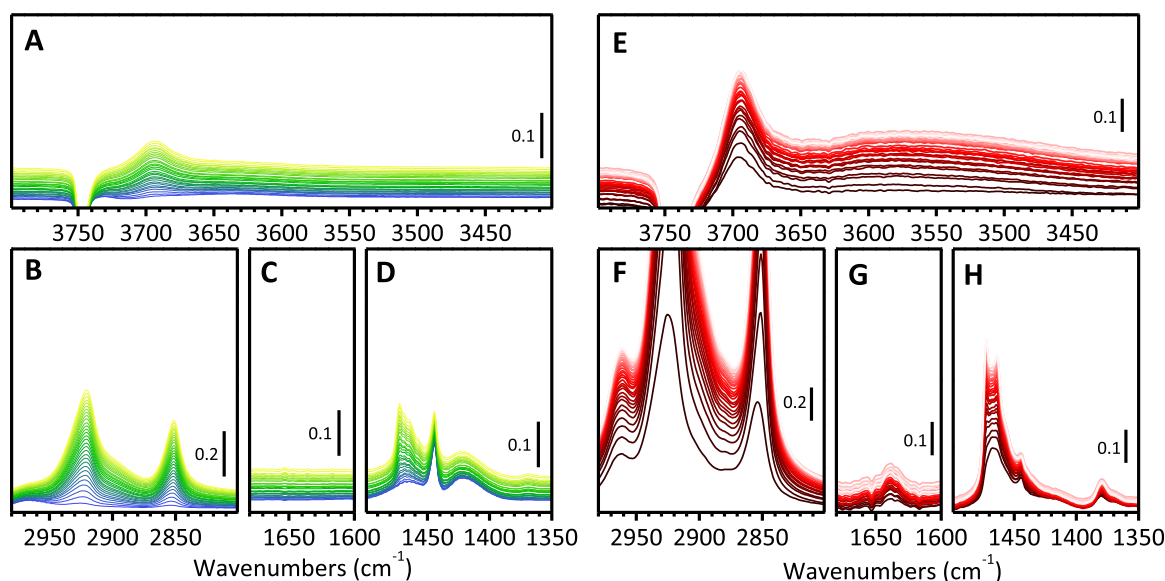
Fig. 14. *Operando* IR spectra collected during ethylene polymerization at room temperature on a standard CO-reduced Cr(II)/SiO$_2$ catalyst (Parta A-D) and on the same system after modification with SiH$_4$ at room temperature (parts E-H). The spectra are reported after subtraction of that collected prior the entrance of ethylene in the reaction cell, in the ν(OH) region (parts A and E), in the ν(CHx) region (parts B and F), in the ν(C═C) region (parts C and G) and in the δ(CH$_x$) region (Parts D and H). In both cases, the last spectrum is collected after 8 min of reaction. All the spectra are normalized to the optical thickness of the pellets. Reproduced from Ref. [202].

very well evident in Fig. 15, which compares the *operando* IR spectra collected during ethylene polymerization at room temperature on two Cr[CH(SiMe$_2$)$_2$]$_3$/SiO$_2$ catalysts, with a chromium loading of 0.2 wt% (part A) and 0.5 wt% (part B), respectively. All the spectroscopic manifestations associated to the formation of α-olefins discussed above are well evident in both sequences of spectra, but especially for the 0.5 wt% loaded catalyst. Opposite to the previous case, where α-olefins were scarcely visible, here they dominate the IR spectra. This indicates that, under the adopted experimental conditions, the rate of α-olefin production is much higher than the rate of their enchainment in the growing
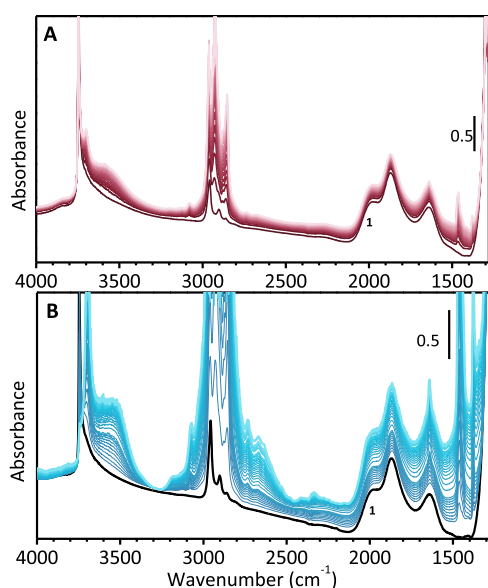

Fig. 15. *Operando* IR spectra collected during ethylene polymerization at room temperature on two Cr[CH(SiMe3)$_2$]$_3$/SiO$_2$ catalysts differing in the chromium loading (0.2 and 0.5 wt%, parts A and B, respectively). In both cases, spectrum 1 was collected before ethene interaction, while the final spectrum was collected after about 20 min of reaction. All the intermediate spectra were collected every 5 s. Reproduced from Ref. [203].

PE.

5.2. Catalytic synergy between Ti(III) and Al(III) sites on a chlorinated Al$_2$O$_3$

A final example of synergy between two different catalytic sites is offered by a bifunctional heterogeneous catalyst obtained by treating a transitional alumina with TiCl$_4$ followed by H$_2$ reduction [206,207]. We demonstrated that this catalyst exposes both Ti(III) and Al(III) Lewis acid sides in close proximity on a highly chlorinated surface, which cooperate to give a branched polyethylene. The structure of the catalyst at a molecular level was deeply investigated by combining several spectroscopic methods. Herein, we report the results obtained by means of *operando* IR spectroscopy, which demonstrates the specific function of each catalytic site.

Fig. 16 shows the sequence of IR spectra collected during the reaction of ethylene on an alumina chlorinated through a treatment in CCl$_4$ at 400 °C, and an analogous experiment performed on the bifunctional TiCl$_4$/Al$_2$O$_3$ catalyst. In the first case, a complex series of absorption bands is observed in the 3000–2800 cm^{-1} (Fig. 16A) and 1600–1300 cm^{-1} (Fig. 16A') regions of the spectra, which are attributed to short and branched oligomers, along with allylic cationic species (band at 1535 cm^{-1}). This indicates the occurrence of an acid-catalysed oligomerization of ethylene, leading to the formation of branched cationic oligomers, likely stabilized by the presence of chloride ions at the catalyst surface. The reaction stops after approximately 30 min. During the first 15 min of reaction on the bifunctional TiCl$_4$/Al$_2$O$_3$ catalyst (Fig. 16B-B'), instead, the IR spectra are very similar to those discussed above, which means that during this time the acid-catalysed formation of branched oligomers prevails. Later on, the spectra evolve differently, with the absorption bands ascribed to vibration of CH$_2$ groups growing faster than those ascribed to vibration of CH$_3$ groups, which indicates the occurrence of ethylene polymerization through a coordination/insertion mechanism at the Ti sites, autonomously continuing for almost one hour (up to the complete consumption of the batch of ethylene).

According to the whole set of spectroscopic data collected on the system, we were able to elucidate that the oligomers produced through a carbocationic mechanism at the exposed Al(III) sites are able to activate
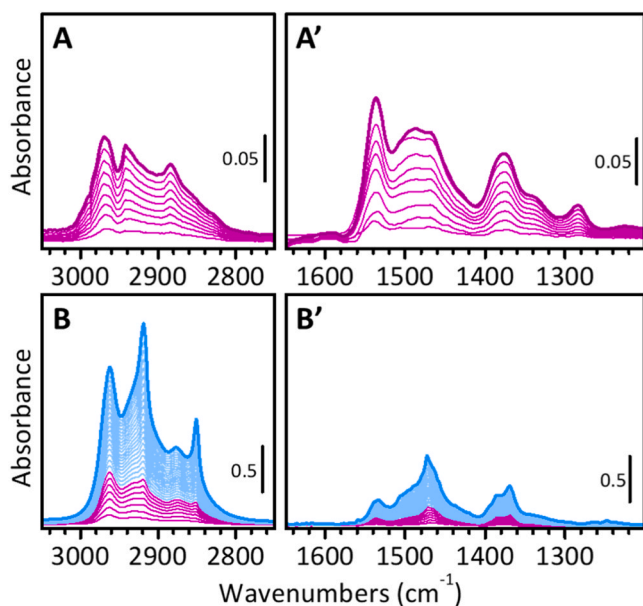
Fig. 16. *Operando* IR spectra, in the ν(CHx) and δ(CHx) spectral regions, collected during oligo/polymerization of ethylene on an alumina chlorinated through a treatment in CCl₄ at 400 °C (parts A and A'), and an analogous experiment performed on the bifunctional TiCl₄/Al₂O₃ catalyst (parts B and B'). The whole sequence of spectra was collected in 60 min. The spectra are reported after subtraction of that collected prior ethylene dosage. Note that the absorbance scale is ten times larger in parts B and B'. Reproduced from Ref. [207].

the surface Ti(III) sites through the double function of dichlorination and alkylation, besides being then incorporated as comonomers in the growing PE chains.

6. Conclusions and perspectives

In this review we have summarized the main results achieved in the field of *operando* spectroscopy applied to different families of heterogeneous catalysts for olefin polymerization. Although the conditions necessary for olefin polymerization are relatively mild (low temperature and low pressure) with respect to many other catalytic processes of industrial interest, application of *operando* spectroscopies to these catalysts has occurred to a lower extent so far. At the beginning, this was mainly due to the difficulties in the manipulation of Al-alkyls by spectroscopists, which explains why for some decades *operando* spectroscopies were almost exclusively applied to the investigation of the Phillips catalyst, the only one which does not require any metal-alkyl cocatalyst to develop activity in the polymerization of ethylene. In the following decades, the ability to manipulate with confidence Al-alkyls also in the laboratories dedicated to spectroscopy, opened the way to the investigation of other families of heterogeneous catalysts, in particular the Ziegler-Natta ones, and more recently also supported metallocene catalysts. Still, the number of research groups actively working in this field is quite limited when compared to other field of catalysis, which mirrors the scarce (even though largely unmotivated) appeal of olefin polymerization catalysis.

This probably explains also why the use of the term *operando* referring to spectroscopy applied to olefin polymerization catalysts is often criticized, even when the measurements are conducted in the presence of the monomer, i.e. on the working catalyst. This is essentially a semantic problem: for most of the researchers used to work in heterogeneous catalysis but not in the field of olefin polymerization, the reactants are in the gas phase and the products are gas or liquids. Hence, the catalyst activity and/or selectivity are determined by measuring the stream out of the reactor cell. In olefin polymerization, instead, the

product is a solid polymer, the activity is evaluated in terms of amount of polymer produced and the concept of selectivity refers to properties of the polymer, such as molecular weight distribution, crystallinity and branches degree for PE, or stereoregularity for PP. However, this does not mean that it is not possible to perform *operando* experiments on this kind of catalysts. Luckily, the spectroscopic fingerprints of the polymer product are often well distinguishable from those of the catalyst, so that during a spectroscopic measurement in the presence of the monomer it is possible to monitor simultaneously the properties of the catalyst and those of the growing polymer. This perfectly fits with the definition of the *operando* approach.

As in many other fields of catalysis, one of the main driving forces for the application of *operando* spectroscopies to olefin polymerisation catalysts is the elucidation of the molecular structure of active sites, as well as the ability to differentiate similar but not equal sites, eventually correlating the structure with the catalytic performances. In this respect, the main lesson that can be extracted from the examples reported in this review is that a unique spectroscopic method usually is not sufficient to disclose the molecular structure of the active sites in these complex catalytic systems. However, relevant results can be obtained by synergistically coupling two or more spectroscopic methods. As far as the differentiation of the active sites is concerned, in this case it is not possible to resort to sophisticated approaches such as modulation-excitation (ME) experiments. In fact, an olefin polymerization catalyst cannot be perturbed periodically, which is at the basis of the ME spectroscopy theory. When the reaction starts, the product of the reaction (i. e., the solid polymer) remains on the catalyst, or better, it encapsulates the catalyst particles, making this strategy inapplicable. However, what can be considered a disadvantage can also be transformed into an advantage. Indeed, in the first instants of the reaction, the only sites that are modified, or even masked by the growing polymer, are the active ones. Therefore, working in difference it is possible to understand which are the spectroscopic fingerprints associated with the active sites, or at least with the first sites that start the reaction. Notable results have been obtained with this approach applied to DR UV-Vis spectroscopy and, more recently, also with X-ray absorption spectroscopy.

Interesting results have also been obtained by applying *operando* IR spectroscopy to trace the polymerization kinetics of similar catalysts tested under similar experimental conditions. It is sufficient to monitor the intensity of the absorption bands associated with the polymer as a function of time to determine the order of the reaction and the kinetic constant. However, the number of active sites is usually not known, so determining the turnover frequency is not trivial, as well as comparing the activity of different catalysts should be done with caution. In this sense, it might be useful to apply the innovative approach based on the use of insertion probes coupled to *operando* IR spectroscopy. This approach, successfully tested so far on some catalysts based on supported metallocenes, permits the quantification of the number of sites capable of coordinating the probe (monomer), as well as to determine the insertion kinetics, without running into diffusion problems associated with the presence of the polymer. By normalizing the overall insertion kinetics to the fraction of sites capable of coordinating the probe (monomer), it is possible to evaluate the intrinsic tendency of the active sites to insert the probe (monomer). The potentials of this approach are still under exploited. Finally, *operando* IR spectroscopy has also proved to be particularly useful for identifying synergistic phenomena between different sites in the same catalyst. The use of tandem catalysts (i.e., containing at least two types of active sites, which perform different functions) is a particularly interesting chapter in the field of polyolefins, because it allows to modulate the properties of the polymer. In the review, some examples of tandem catalysts were reported, displaying that it is possible, starting from a feed of only ethylene, to produce a low density PE similar to that obtained in the presence of α-olefins as comonomers.

The examples reported in this review demonstrate the enormous potential of *operando* spectroscopies in the field of olefin polymerization

catalysis. It is important to continue to contribute in this area, ideally with the support of the companies involved, so as to progress and stimulate the development of new experimental set-ups, approaches, and solutions.

CRediT authorship contribution statement

Groppo Elena: Conceptualization, Data curation, Funding acquisition, Methodology, Supervision, Validation, Visualization, Writing – original draft. **Piovano Alessandro:** Data curation, Formal analysis, Investigation, Methodology, Writing – review & editing.

Declaration of Competing Interest

The authors declare that they have no known competing financial interests or personal relationships that could have appeared to influence the work reported in this paper.

Data availability

Data will be made available on request.

Acknowledgments

References

[1] T.E. Nowlin. Business and Technology of the Global Polyethylene Industry: An In-depth Look at the History, Technology, Catalysts, and Modern Commercial Manufacture of Polyethylene and Its Products, Scrivener Publishing LLC, Wiley, New York, 2014.

[2] J. Jansz, in: Global PO&E News Analysis, Chemical Market Resources, Inc., 2015.

[3] C. Chen, Designing catalysts for olefin polymerization and copolymerization: beyond electronic and steric tuning, Nat. Rev. Chem. 2 (2018) 6–14.

[4] G. Antinucci, R. Cipullo, V. Busico, Imagine polypropylene, Nat. Catal. 6 (2023) 456–457.

[5] W. Kaminsky, Polyolefins: 50 years after Ziegler and Natta I: Polyethylene and Polypropylene, Springer, Heidelberg, 2013.

[6] V. Busico, Metal-catalysed olefin polymerisation into the new millennium: a perspective outlook, Dalton Trans. (2009) 8794–8802.

[7] V. Busico, Ziegler-natta catalysis: forever young, Mrs Bull. 38 (2013) 224–228.

[8] J.C. Chadwick, Polyolefins - catalyst and process innovations and their impact on polymer properties, Macromol. React. Eng. 3 (2009) 428–432.

[9] J. Qiao, M. Guo, L. Wang, D. Liu, X. Zhang, L. Yu, W. Song, Y. Liu, Recent advances in polyolefin technology, Polym. Chem. 2 (2011) 1611–1623.

[10] P.S. Chum, K.W. Swogger, Olefin polymer technologies—history and recent progress at the dow chemical company, Prog. Polym. Sci. 33 (2008) 797–819.

[11] M. Gahleitner, L. Resconi, P. Doshev, Heterogeneous Ziegler-Natta, metallocene, and post-metallocene catalysis: Successes and challenges in industrial application, MRS Bull. 38 (2013) 229–233.

[12] L.L. Böhm, The ethylene polymerization with Ziegler catalysts: fifty years after the discovery, Angew. Chem. -Int. Ed. 42 (2003) 5010–5030.

[13] M. Stürzel, S. Mihan, R. Mülhaupt, From multisite polymerization catalysis to sustainable materials and all-polyolefin composites, Chem. Rev. 116 (2016) 1398–1433.

[14] M.D. Tabone, J.J. Cregg, E.J. Beckman, A.E. Landis, Sustainability metrics: life cycle assessment and green design in polymers, Environ. Sci. Technol. 44 (2010) 8264–8269.

[15] R. Mülhaupt, Green polymer chemistry and bio-based plastics: dreams and reality, Macromol. Chem. Phys. 214 (2013) 159–174.

[16] M.A. Dubé, S. Salehpour, Applying the principles of green chemistry to polymer production technology, Macromol. React. Eng. 8 (2014) 7–28.

[17] J.R. Severn, J.C. Chadwick, R. Duchateau, N. Friederichs, Bound but not gagged" - Immobilizing single-site α-olefin polymerization catalysts, Chem. Rev. 105 (2005) 4073–4147.

[18] J.B.P. Soares, T.F.L. McKenna, Polyolefin Reaction Engineering, Wiley-VCH, Weinheim, Germany, 2012.

[19] L. Jasinska-Walc, M. Bouyahyi, R. Duchateau, Potential of functionalized polyolefins in a sustainable polymer economy: synthetic strategies and applications, Acc. Chem. Res. 55 (2022) 1985–1996.

[20] A. Macchioni, Ion pairing in transition-metal organometallic chemistry, Chem. Rev. 105 (2005) 2039–2073.

[21] F. Zaccaria, L. Sian, C. Zuccaccia, A. Macchioni, Chapter One - Ion pairing in transition metal catalyzed olefin polymerization, in: P.J. Pérez (Ed.), Advances in Organometallic Chemistry, Academic Press, 2020, pp. 1–78.

[22] R. Credendino, D. Liguori, Z. Fan, G. Morini, L. Cavallo, Toward a unified model explaining heterogeneous ziegler-Natta catalysis, ACS Catal. 5 (2015) 5431–5435.

[23] C. Barzan, A. Piovano, L. Braglia, G.A. Martino, C. Lamberti, S. Bordiga, E. Groppo, Ligands make the difference! molecular insights into CrVI/SiO2 Phillips catalyst during ethylene polymerization, J. Am. Chem. Soc. 139 (2017) 17064–17073.

[24] A. Piovano, E. Groppo, Flexible ligands in heterogeneous catalysts for olefin polymerization: insights from spectroscopy, Coord. Chem. Rev. 451 (2022), 214258.

[25] M.A. Bañares, Operando methodology: combination of in situ spectroscopy and simultaneous activity measurements under catalytic reaction conditions, Catal. Today 100 (2005) 71–77.

[26] B.M. Weckhuysen, Determining the active site in a catalytic process: operando spectroscopy is more than a buzzword, Phys. Chem. Chem. Phys. 5 (2003) 4351–4360.

[27] H. Topsøe, Developments in operando studies and in situ characterization of heterogeneous catalysts, J. Catal. 216 (2003) 155–164.

[28] M.P. McDaniel, Supported chromium catalysts for ethylene polymerization, Adv. Catal. 33 (1985) 47–98.

[29] M.P. McDaniel, Handbook of heterogeneous catalysis, in: G. Ertl, H. Knözinger, J. Weitkamp (Eds.), Handbook of heterogeneous catalysis, VHC, Weinheim, 1997, p. 2400.

[30] M.P. McDaniel, A review of the Phillips supported chromium catalyst and its commercial use for ethylene polymerization, : Adv. Catal. (2010) 123–606.

[31] M.P. McDaniel, A review of the Phillips Chromium Catalyst for Ethylene Polymerization, Handbook of Transition Metal Polymerization Catalysts: Second Edition, (2018) 401–571.

[32] E. Groppo, C. Lamberti, S. Bordiga, G. Spoto, A. Zecchina, The structure of active centers and the ethylene polymerization mechanism on the Cr/SiO₂ catalyst: a frontier for the characterization methods, Chem. Rev. 105 (2005) 115–184.

[33] E. Groppo, G.A. Martino, A. Piovano, C. Barzan, The Active Sites in the Phillips Catalysts: Origins of a Lively Debate and a Vision for the Future, in: ACS Catalysis, American Chemical Society, 2018, pp. 10846–10863.

[34] E. Groppo, K. Seenivasan, C. Barzan, The potential of spectroscopic methods applied to heterogeneous catalysts for olefin polymerization, Catal. Sci. Technol. 3 (2013) 858–878.

[35] B.M. Weckhuysen, I.E. Wachs, R.A. Schoonheydt, Surface chemistry and spectroscopy of chromium in inorganic oxides, Chem. Rev. 96 (1996) 3327–3349.

[36] R. Cheng, Z. Liu, L. Zhong, X. He, P. Qiu, M. Terano, M.S. Eisen, S.L. Scott, B. Liu, Phillips Cr/Silica Catalyst for Ethylene Polymerization, in: W. Kaminsky (Ed.), Polyolefins: 50 years after Ziegler and Natta I, Springer Berlin Heidelberg, Berlin, Heidelberg, 2013, pp. 135–202.

[37] C. Brown, J. Krzystek, R. Achey, A. Lita, R. Fu, R.W. Meulenberg, M. Polinski, N. Peek, Y. Wang, L.J. Van De Burgt, S. Profeta, A.E. Stiegman, S.L. Scott, Mechanism of Initiation in the Phillips Ethylene Polymerization Catalyst: Redox Processes Leading to the Active Site, ACS Catal. 5 (2015) 5574–5583.

[38] C. Brown, A. Lita, Y. Tao, N. Peek, M. Crosswhite, M. Mileham, J. Krzystek, R. Achey, R. Fu, J.K. Bindra, M. Polinski, Y. Wang, L.J. Van De Burgt, D. Jeffcoat, S. Profeta, A.E. Stiegman, S.L. Scott, Mechanism of initiation in the Phillips ethylene polymerization catalyst: ethylene activation by Cr(II) and the structure of the resulting active site, ACS Catal. 7 (2017) 7442–7455.

[39] A. Fong, Y. Yuan, S.L. Ivry, S.L. Scott, B. Peters, Computational kinetic discrimination of ethylene polymerization mechanisms for the Phillips (Cr/SiO2) catalyst, ACS Catal. 5 (2015) 3360–3374.

[40] A. Fong, B. Peters, S.L. Scott, One-electron-redox activation of the reduced Phillips polymerization catalyst, via alkylchromium(IV) homolysis: a computational assessment, ACS Catal. 6 (2016) 6073–6085.

[41] A. Fong, C. Vandervelden, S.L. Scott, B. Peters, Computational support for Phillips catalyst initiation via Cr-c bond homolysis in a chromacyclopentane site, ACS Catal. 8 (2018) 1728–1733.

[42] B. Peters, S.L. Scott, A. Fong, Y. Wang, A.E. Stiegman, Reexamining the evidence for proton transfers in ethylene polymerization, Proc. Natl. Acad. Sci. USA 112 (2015) E4160–E4161.

[43] M.P. Conley, M.F. Delley, G. Siddiqi, G. Lapadula, S. Norsic, V. Monteil, O. V. Safonova, C. Copéret, Polymerization of ethylene by silica-supported dinuclear CrIII sites through an initiation step involving C═H bond activation, Angew. Chem. Int. Ed. 53 (2014) 1872–1876.

[44] M.P. Conley, M.F. Delley, F. Núñez-Zarur, A. Comas-Vives, C. Copéret, Heterolytic activation of C-H bonds on CrIII-O surface sites is a key step in catalytic polymerization of ethylene and dehydrogenation of propane, Inorg. Chem. 54 (2015) 5065–5078.

[45] M.P. Conley, M.F. Delley, G. Siddiqi, G. Lapadula, S. Norsic, V. Monteil, O.V. Safonova, C. Copéret, Erratum: Polymerization of ethylene by silica-supported dinuclear CrIII sites through an initiation step involving C-H bond activation (Angewandte Chemie - International Edition (2014) (53)), in: Angewandte Chemie - International Edition, Wiley-VCH Verlag, 2015, pp. 6670–6670.

[46] M.F. Delley, F. Núñez-Zarur, M.P. Conley, A. Comas-Vives, G. Siddiqi, S. Norsic, V. Monteil, O.V. Safonova, C. Copéret, Proton transfers are key elementary steps in ethylene polymerization on isolated chromium(III) silicates, Proc. Natl. Acad. Sci. USA 111 (2014) 11624–11629.

[47] M.F. Delley, M.P. Conley, C. Copéret, Polymerization on CO-reduced Phillips catalyst initiates through the C-H bond activation of ethylene on Cr-O sites, Catal. Lett. 144 (2014) 805–808.

[48] M.F. Delley, F. Nuñez-Zarura, M.P. Conley, A. Comas-Vivesa, G. Siddiqia, S. Norsic, V. Monteil, O.V. Safonova, C. Copéret, Reply to Peters et al.: Proton transfers are plausible initiation and termination steps on Cr(III) in ethylene polymerization, in: Proceedings of the National Academy of Sciences of the United States of America, National Academy of Sciences, 2015, pp. E4162-E4163.

[49] D.S. McGuinness, N.W. Davies, J. Horne, I. Ivanov, Unraveling the mechanism of polymerization with the phillips catalyst, Organometallics 29 (2010) 6111–6116.

[50] C.A. Cruz, M.M. Monwar, J. Barr, M.P. McDaniel, Identification of the starting group on the first pe chain produced by the phillips catalyst, Macromolecules 52 (2019) 5750–5760.

[51] C. Lamberti, E. Groppo, G. Spoto, S. Bordiga, A. Zecchina, Infrared spectroscopy of surface transient species, Adv. Catal. 51 (2007) 1–74.

[52] G. Ghiotti, E. Garrone, A. Zecchina, IR investigation of polymerization centres of the Phillips, Catal., J. Mol. Catal. 46 (1988) 61–77.

[53] G. Spoto, S. Bordiga, E. Garrone, G. Ghiotti, A. Zecchina, G. Petrini, G. Leofanti, Cr(II) and Cr(III) ions grafted at internal nests of a pentasilic zeolite (silicalite) - characterization and formation of polycarbonylic, polynitrosylic, and mixed species by interaction with CO and NO, J. Mol. Catal. 74 (1992) 175–184.

[54] A. Zecchina, G. Spoto, G. Ghiotti, E. Garrone, Cr2+ ions grafted to silica and silicalite surfaces: FTIR characterization and ethylene polymerization activity, J. Mol. Catal. 86 (1994) 423–446.

[55] S. Bordiga, S. Bertarione, A. Damin, C. Prestipino, G. Spoto, C. Lamberti, A. Zecchina, On the first stages of the ethylene polymerization on Cr2+/SiO2 Phillips catalyst: time and temperature resolved IR, Stud., J. Mol. Catal. A 204 (2003) 527–534.

[56] K. Vikulov, G. Spoto, S. Coluccia, A. Zecchina, FTIR investigation of ethylene coordination and polymerization on reduced Cr/SiO2 catalyst, Catal. Lett. 16 (1992) 117–122.

[57] O.M. Bade, R. Blom, I.M. Dahl, A. Karlsson, A. DRIFTS, study of the Cr(II)/SiO2 catalyst - Ethylene coordination and early stages of polymerisation, J. Catal. 173 (1998) 460–469.

[58] E. Groppo, C. Lamberti, S. Bordiga, G. Spoto, A. Damin, A. Zecchina, FTIR investigation of the H2, N2, and C 2H4 molecular complexes formed on the Cr(II) sites in the Phillips catalyst: A preliminary step in the understanding of a complex system, J. Phys. Chem. B 109 (2005) 15024–15031.

[59] E. Groppo, C. Lamberti, S. Bordiga, G. Spoto, A. Zecchina, In situ FTIR spectroscopy of key intermediates in the first stages of ethylene polymerization on the Cr/SiO2 Phillips catalyst: Solving the puzzle of the initiation mechanism? J. Catal. 240 (2006) 172–181.

[60] D.S. McGuinness, Olefin oligomerization via metallacycles: dimerization, trimerization, tetramerization, and beyond, Chem. Rev. 111 (2011) 2321–2341.

[61] A. Jabri, C.B. Mason, Y. Sim, S. Gambarotta, T.J. Burchell, R. Duchateau, Isolation of single-component trimerization and polymerization chromium catalysts: the role of the metal oxidation state, Angew. Chem. -Int. Ed. 47 (2008) 9717–9721.

[62] I. Thapa, S. Gambarotta, I. Korobkov, M. Murugesu, P. Budzelaar, Isolation and characterization of a class II mixed-valence chromium(I)/(II) self-activating ethylene trimerization catalyst, Organometallics 31 (2012) 486–494.

[63] B.M. Weckhuysen, R.A. Schoonheydt, J.M. Jehng, I.E. Wachs, S.J. Cho, R. Ryoo, S. Kijlstra, E. Poels, Combined DRS-RS-EXAFS-XANES-, TPR Study Support. Chromium Catal., J. Chem. Soc. Faraday Trans. 91 (1995) 3245–3253.

[64] E. Groppo, C. Prestipino, F. Cesano, F. Bonino, S. Bordiga, C. Lamberti, P. C. Thüne, J.W. Niemantsverdriet, A. Zecchina, In situ, Cr K-edge XAS study on the Phillips catalyst: activation and ethylene polymerization, J. Catal. 230 (2005) 98–108.

[65] S. Bordiga, E. Groppo, G. Agostini, J.A. Van Bokhoven, C. Lamberti, Reactivity of surface species in heterogeneous catalysts probed by in situ x-ray absorption techniques, Chem. Rev. 113 (2013) 1736–1850.

[66] G. Agostini, E. Groppo, S. Bordiga, A. Zecchina, C. Prestipino, F. D'Acapito, E. Van Kimmenade, P.C. Thüne, J.W. Niemantsverdriet, C. Lamberti, Reactivity of Cr species grafted on SiO2/Si(100) surface: A reflection extended X-ray absorption fine structure study down to the submonolayer regime, J. Phys. Chem. C. 111 (2007) 16437–16444.

[67] D. Gianolio, E. Groppo, J.G. Vitillo, A. Damin, S. Bordiga, A. Zecchina, C. Lamberti, Direct evidence of adsorption induced CrII mobility on the SiO2 surface upon complexation by CO, Chem. Commun. 46 (2010) 976–978.

[68] L. Zhong, M.Y. Lee, Z. Liu, Y.J. Wanglee, B. Liu, S.L. Scott, Spectroscopic and structural characterization of Cr(II)/SiO2 active site precursors in model Phillips polymerization catalysts, J. Catal. 293 (2012) 1–12.

[69] M. Botavina, C. Barzan, A. Piovano, L. Braglia, G. Agostini, G. Martra, E. Groppo, Insights into Cr/SiO2 catalysts during dehydrogenation of propane: an operando XAS investigation, Catal. Sci. Technol. 7 (2017) 1690–1700.

[70] D. Trummer, K. Searles, A. Algasov, S.A. Guda, A.V. Soldatov, H. Ramanantoanina, O.V. Safonova, A.A. Guda, C. Copéret, Deciphering the Phillips Catalyst by Orbital Analysis and Supervised Machine Learning from Cr Pre-edge XANES of Molecular Libraries, J. Am. Chem. Soc. 143 (2021) 7326–7341.

[71] M. Tromp, J.O. Moulin, G. Reid, J. Evans, Cr K-edge XANES spectroscopy: ligand and oxidation state dependence - What is oxidation state?, AIP Conf. Proc., 882 (2007) 699–701.

[72] B.M. Weckhuysen, L.M. Deridder, R.A. Schoonheydt, A quantitative diffuse reflectance spectroscopy study of supported chromium catalysts, J. Phys. Chem. 97 (1993) 4756–4763.

[73] B.M. Weckhuysen, A.A. Verberckmoes, A.L. Buttiens, R.A. Schoonheydt, Diffuse reflectance spectroscopy study of the thermal genesis and molecular structure of chromium-supported catalysts, J. Phys. Chem. 98 (1994) 579–584.

[74] B.M. Weckhuysen, L.M. De Ridder, P.J. Grobet, R.A. Schoonheydt, Redox behavior and dispersion of supported chromium catalysts, J. Phys. Chem. 99 (1995) 320–326.

[75] B.M. Weckhuysen, B. Schoofs, R.A. Schoonheydt, Mobility of chromium in inorganic oxides - Spectroscopic fingerprinting of oxidation states and coordination environments, J. Chem. Soc. Faraday Trans. 93 (1997) 2117–2120.

[76] B.M. Weckhuysen, A.A. Verberckmoes, A.R. De Baets, R.A. Schoonheydt, Diffuse reflectance spectroscopy of supported chromium oxide catalysts: a self-modeling mixture analysis, J. Catal. 166 (1997) 160–171.

[77] B.M. Weckhuysen, R.A. Schoonheydt, Recent progresses in diffuse reflectance spectroscopy of supported metal oxide catalysts, Catal. Today 49 (1999) 441–451.

[78] B.M. Weckhuysen, A.A. Verberckmoes, J. Debaere, K. Ooms, I. Langhans, R. A. Schoonheydt, In situ UV-Vis diffuse reflectance spectroscopy - On line activity measurements of supported chromium oxide catalysts: Relating isobutane dehydrogenation activity with Cr-speciation via experimental design, J. Mol. Catal. A: Chem. 151 (2000) 115–131.

[79] E. Morra, G.A. Martino, A. Piovano, C. Barzan, E. Groppo, M. Chiesa, In Situ X- and Q-Band EPR Investigation of Ethylene Polymerization on Cr/SiO2 Phillips Catalyst, J. Phys. Chem. C. 122 (2018) 21531–21536.

[80] E. Groppo, C. Lamberti, G. Spoto, S. Bordiga, G. Magnacca, A. Zecchina, Tuning the structure, distribution and reactivity of polymerization centres of Cr(II)/SiO2 Phillips catalyst by controlled annealing, J. Catal. 236 (2005) 233–244.

[81] C. Barzan, S. Bordiga, E. Groppo, Toward the understanding of the comonomer effect on CrII/SiO2 Phillips catalyst, ACS Catal. 6 (2016) 2918–2922.

[82] K.C. Potter, C.W. Beckerle, F.C. Jentoft, E. Schwerdtfeger, M.P. McDaniel, Reduction of the Phillips catalyst by various olefins: stoichiometry, thermochemistry, reaction products and polymerization activity, J. Catal. 344 (2016) 657–668.

[83] E. Schwerdtfeger, R. Buck, M. McDaniel, Reduction of Cr(VI) polymerization catalysts by non-olefinic hydrocarbons, Appl. Catal. A 423-424 (2012) 91–99.

[84] Z. Liu, X. He, R. Cheng, M.S. Eisen, M. Terano, S.L. Scott, B. Liu, Chromium catalysts for ethylene polymerization and oligomerization, in: advances in Chemical Engineering, Acad. Press Inc. (2014) 127–191.

[85] B. Liu, H. Nakatani, M. Terano, New aspects of the induction period of ethene polymerization using Phillips CrO x /SiO 2 catalyst probed by XPS, TPD and EPMA, in: Journal of Molecular Catalysis A: Chemical, 2002, pp. 387–398.

[86] B. Liu, H. Nakatani, M. Terano, Mechanistic implications of the unprecedented transformations of ethene into propene and butene over Phillips CrOx/SiO2 catalyst during induction period, J. Mol. Catal. A: Chem. 201 (2003) 189–197.

[87] W. Xia, B. Liu, Y. Fang, K. Hasebe, M. Terano, Unique polymerization kinetics obtained from simultaneous interaction of Phillips Cr(VI)Ox/SiO2 catalyst with Al-alkyl cocatalyst and ethylene monomer, J. Mol. Catal. A: Chem. 256 (2006) 301–308.

[88] L. Zhong, Z. Liu, R. Cheng, S. Tang, P. Qiu, X. He, M. Terano, B. Liu, Active site transformation during the induction period of ethylene polymerization over the Phillips CrOx/SiO2 catalyst, ChemCatChem 4 (2012) 872–881.

[89] C. Barzan, A.A. Damin, A. Budnyk, A. Zecchina, S. Bordiga, E. Groppo, Pre-reduction of the Phillips CrVI/SiO2 catalyst by cyclohexene: a model for the induction period of ethylene polymerization, J. Catal. 337 (2016) 45–51.

[90] V. Crocellà, G. Cerrato, G. Magnacca, C. Morterra, F. Cavani, L. Maselli, S. Passeri, Gas-phase phenol methylation over Mg/Me/O (Me = Al, Cr, Fe) catalysts: mechanistic implications due to different acid-base and dehydrogenating properties, Dalton Trans. 39 (2010) 8527–8537.

[91] G.J. Millar, C.H. Rochester, K.C. Waugh, Infrared study of methyl formate and formaldehyde adsorption on reduced silica-supported copper catalysts, J. Chem. Soc., Faraday Trans. 87 (1991) 2785–2793.

[92] G.J. Millar, C.H. Rochester, K.C. Waugh, Evidence for the adsorption of molecules at special sites located at copper/zinc oxide interfaces. Part 3.—Fourier-transform infrared study of methyl formate adsorption on reduced and oxidised Cu/ZnO/ SiO2 catalysts, J. Chem. Soc., Faraday Trans. 88 (1992) 3497–3503.

[93] L. Mino, C. Barzan, G.A. Martino, A. Piovano, G. Spoto, A. Zecchina, E. Groppo, Photoinduced Ethylene Polymerization on the Cr VI /SiO 2 Phillips Catalyst, J. Phys. Chem. C. 123 (2019) 8145–8152.

[94] E. Groppo, J. Estephane, C. Lamberti, G. Spoto, A. Zecchina, Ethylene, propylene and ethylene oxide in situ polymerization on the Cr(II)/SiO2 system: A temperature- and pressure-dependent investigation, Catal. Today 126 (2007) 228–234.

[95] A. Andoni, J.C. Chadwick, H.J.W. Niemantsverdriet, P.C. Thune, A preparation method for well-defined crystallites of Mgcl(2)-supported Ziegler-Natta catalysts and their observation by AFM and SEM, Macromol. Rapid Commun. 28 (2007) 1466–1471.

[96] A. Andoni, J.C. Chadwick, S. Milani, H. Niemantsverdriet, P.C. Thune, Introducing a new surface science model for Ziegler-Natta catalysts: Preparation, basic characterization and testing, J. Catal. 247 (2007) 129–136.

[97] A. Andoni, J.C. Chadwick, H.J.W. Niemantsverdriet, P.C. Thune, The Role of Electron Donors on Lateral Surfaces of MgCl2-Supported Ziegler-Natta Catalysts: Observation by AFM and SEM, J. Catal. 257 (2008) 81–86.

[98] A. Andoni, J.C. Chadwick, J.W. Niemantsverdriet, P.C. Thune, Investigation of Planar Ziegler-Natta Model Catalysts Using Attenuated Total Reflection Infrared Spectroscopy, Catal. Lett. 130 (2009) 278–285.

[99] A.V. Cheruvathur, E.H.G. Langner, J.W. Niemantsverdriet, P.C. Thüne, In Situ ATR-FTIR Studies on MgCl2-Diisobutyl Phthalate Interactions in Thin Film Ziegler-Natta Catalysts, Langmuir 28 (2012) 2643–2651.

[100] P.C. Thune, C.P.J. Verhagen, M.J.G. van den Boer, J.W. Niemantsverdriet, Working surface science model for the Phillips ethylene polymerization catalyst: Preparation and testing, J. Phys. Chem. B 101 (1997) 8559–8563.

[101] P.C. Thune, J. Loos, P.J. Lemstra, J.W. Niemantsverdriet, Polyethylene formation on a planar surface science model of a chromium oxide polymerization catalyst, J. Catal. 183 (1999) 1–5.

[102] P.C. Thune, J. Loos, A.M. de Jong, P.J. Lemstra, J.W. Niemantsverdriet, Planar model system for olefin polymerization: the Phillips CrOₓ/SiO₂ catalyst, Top. Catal. 13 (2000) 67–74.

[103] P.C. Thune, R. Linke, W.J.H. van Gennip, A.M. de Jong, J.W. Niemantsverdriet, Bonding of supported chromium during thermal activation of the CrOₓ/SiO₂ (Phillips) ethylene polymerization catalyst, J. Phys. Chem. B 105 (2001) 3073–3078.

[104] P.C. Thune, J. Loos, D. Wouters, P.J. Lemstra, J.W. Niemantsverdriet, The CrOₓ/SiO₂/Si(100) catalyst - A surface science approach to supported olefin polymerization catalysis, Macromol. Symp. 173 (2001) 37–52.

[105] P.C. Thune, J. Loos, X.H. Chen, E.M.E. van Kimmenade, B. Kong, J.W. H. Niemantsverdriet, Visualization of local ethylene polymerization activity on a flat CrOx/SiO2/Si(100) model catalyst, Top. Catal. 46 (2007) 239–245.

[106] P.C. Thüne, J. Loos, A.M. De Jong, P.J. Lemstra, J.W. Niemantsverdriet, Planar model system for olefin polymerization: the Phillips CrO x /SiO 2 catalyst, in: Topics in Catalysis, 2000.

[107] P.C. Thüne, R. Linke, W.J.H. Van Gennip, A.M. De Jong, J.W. Niemantsverdriet, Bonding of supported chromium during thermal activation of the CrOx/SiO2 (Phillips) ethylene polymerization catalyst, J. Phys. Chem. B 105 (2001) 3073–3078.

[108] E.M.E. van Kimmenade, A.E.T. Kuiper, Y. Tamminga, P.C. Thune, J. W. Niemantsverdriet, A surface science model for the Phillips ethylene polymerization catalyst: thermal activation and polymerization activity, J. Catal. 223 (2004) 134–141.

[109] E.M.E. van Kimmenade, J. Loos, J.W. Niemantsverdriet, P.C. Thune, The effect of temperature on ethylene polymerization over flat Phillips model catalysts, J. Catal. 240 (2006) 39–46.

[110] M. D'Amore, K.S. Thushara, A. Piovano, M. Causà, S. Bordiga, E. Groppo, Surface investigation and morphological analysis of structurally disordered MgCl2 and MgCl2/TiCl4 Ziegler-natta catalysts, ACS Catal. 6 (2016) 5786–5796.

[111] A. Piovano, G.A. Martino, C. Barzan, A spectroscopic investigation of silica-supported TiClx species: a case study towards Ziegler-Natta catalysis, Rend. Fis. Acc. Lince-.-. 28 (2017) 43–49.

[112] A. Piovano, M. D'Amore, K.S. Thushara, E. Groppo, Spectroscopic Evidences for TiCl4/Donor Complexes on the Surface of MgCl2-Supported Ziegler-Natta Catalysts, J. Phys. Chem. C 122 (2018) 5615–5626.

[113] A. Piovano, P. Pletcher, M.E.Z. Velthoen, S. Zanoni, S.-H. Chung, K. Bossers, M. K. Jongkind, G. Fiore, E. Groppo, B.M. Weckhuysen, Genesis of MgCl2-based Ziegler-Natta Catalysts as Probed with Operando Spectroscopy, ChemPhysChem 19 (2018) 2662–2671.

[114] K.S. Thushara, M. D'Amore, A. Piovano, S. Bordiga, E. Groppo, The influence of alcohols in driving the morphology of magnesium chloride nanocrystals, ChemCatChem 9 (2017) 1782–1787.

[115] P. Pletcher, A. Welle, A. Vantomme, B.M. Weckhuysen, Quality control for Ziegler-Natta catalysis via spectroscopic fingerprinting, J. Catal. 363 (2018) 128–135.

[116] K.W. Bossers, L.D.B. Mandemaker, N. Nikolopoulos, Y. Liu, M. Rohnke, P. de Peinder, B.J.P. Terlingen, F. Walther, J.M. Dorresteijn, T. Hartman, B. M. Weckhuysen, A. Ziegler-type, spherical cap model reveals early stage ethylene polymerization growth versus catalyst fragmentation relationships, Nature, Communications 13 (2022) 4954.

[117] A. Piovano, T. Wada, A. Amodio, G. Takasao, T. Ikeda, D. Zhu, M. Terano, P. Chammingkwan, E. Groppo, T. Taniike, Formation of highly active ziegler–natta catalysts clarified by a multifaceted characterization approach, ACS, Catalysis 11 (2021) 13782–13796.

[118] A.G. Potapov, G.D. Bukatov, V.A. Zakharov, DRIFT study of internal donors in supported Ziegler-Natta, Catal., J. Mol. Catal. A: Chem. 246 (2006) 248–254.

[119] A.G. Potapov, G.D. Bukatov, V.A. Zakharov, DRIFTS study of the interaction of the AlEt3 cocatalyst with the internal donor ethyl benzoate in supported Ziegler-Natta, Catal., J. Mol. Catal. A: Chem. 301 (2009) 18–23.

[120] A.G. Potapov, G.D. Bukatov, V.A. Zakharov, DRIFTS Study of the Interaction of the Internal Donor in TiCl4/di-n-Butyl Phthalate/MgCl2 Catalysts with AlEt3 Cocatalyst, J. Mol. Catal. A: Chem. 316 (2010) 95–99.

[121] D.V. Stukalov, V.A. Zakharov, A.G. Potapov, G.D. Bukatov, Supported Ziegler-Natta catalysts for Propylene Polymerization. Study of Surface Species Formed at Interaction of Electron Donors and TiCl4 with Activated MgCl2, J. Catal. 266 (2009) 39–49.

[122] L. Brambilla, G. Zerbi, F. Piemontesi, S. Nascetti, G. Morini, Structure of MgCl2-TiCl4 complex in co-milled Ziegler-Natta catalyst precursors with different TiCl4 content: Experimental and theoretical vibrational spectra, J. Mol. Catal. A-Chem. 263 (2007) 103–111.

[123] L. Brambilla, G. Zerbi, F. Piemontesi, S. Nascetti, G. Morini, Structure of Donor Molecule 9,9-Bis(Methoxymethyl)-Fluorene in Ziegler-Natta Catalyst by Infrared Spectroscopy and Quantum Chemical Calculation, J. Phys. Chem. C. 114 (2010) 11475–11484.

[124] M. Terano, T. Kataoka, T. Keii, Analytical and kinetic approaches for the basic type of Mgcl2-supported high-yield, Catal., J. Polym. Sci. Pol. Chem. 28 (1990) 2035–2048.

[125] V. Di Noto, D. Fregonese, A. Marigo, S. Bresadola, High Yield MgCl2-supported catalysts for propene polymerization: effects of ethyl propionate as internal donor on the activity and stereospecificity, Macromol. Chem. Phys. 199 (1998) 633–640.

[126] V.H. Nissinen, M. Linnolahti, A.S. Bazhenov, T.T. Pakkanen, T.A. Pakkanen, P. Denifl, T. Leinonen, K. Jayaratne, A. Pakkanen, Polyethylenimines: multidentate electron donors for Ziegler–Natta catalysts, The, J. Phys. Chem. C. 121 (2017) 23413–23421.

[127] P. Valsesia, M. Beretta, S. Bracco, A. Comotti, P. Sozzani, Polymer/silica nanocomposite micro-objects as a key point for silica-to-polymer shape replication, J. Mater. Chem. 18 (2008) 5511–5517.

[128] T. McKenna, A. Martino, G. Weickert, J. Soares, Particle growth during the polymerisation of olefins on supported catalysts, 1 – nascent polymer structures, Macromol. React. Eng. 4 (2010) 40–64.

[129] A. Bashir, T. McKenna, Reaction Engineering of Polyolefins: The Role of Catalyst Supports in Ethylene Polymerization on Metallocene Catalysts, in (2017) 19–63.

[130] E. Groppo, K. Seenivasan, E. Gallo, A. Sommazzi, C. Lamberti, S. Bordiga, Activation and In Situ Ethylene Polymerization on Silica-Supported Ziegler-Natta Catalysts, ACS Catal. 5 (2015) 5586–5595.

[131] F.J. Karol, Studies with High Activity Catalysts for Olefin Polymerization, Catal. Rev.: Sci. Eng. 26 (1984) 557–595.

[132] T.E. Nowlin, R.I. Mink, Y.V. Kissin, Supported Magnesium/Titanium-Based Ziegler Catalysts for Production of Polyethylene, in: R. Hoff, R.T. Mathers (Eds.), Transition Metal Polymerization Catalysts, John Wiley & Sons, Hoboken (New Jersey), 2009, pp. 131–155.

[133] Y.V. Kissin, Alkene Polymerization Reactions with Transition Metal Catalysts, Elsevier,, Amsterdam, 2008.

[134] K. Seenivasan, A. Sommazzi, F. Bonino, S. Bordiga, E. Groppo, Spectroscopic Investigation of Heterogeneous Ziegler-Natta Catalysts: Ti and Mg Chloride Tetrahydrofuranates, Their Interaction Compound, and the Role of the Activator, Chem. Eur. J. 17 (2011) 8648–8656.

[135] E. Groppo, E. Gallo, K. Seenivasan, A. Sommazzi, S. Bordiga, P. Glatzel, R. Van Silfhout, A. Kachatkou, W. Bras, C. Lamberti, XAS and XES techniques shed light on the dark side of Ziegler-Natta catalysts: active sites generation, ChemCatChem 7 (2015) 1432–1437.

[136] V. D'Anna, S. Norsic, D. Gajan, K. Sanders, A.J. Pell, A. Lesage, V. Monteil, C. Copéret, G. Pintacuda, P. Sautet, Structural Characterization of the EtOH-TiCl4-MgCl2 Ziegler-Natta Precatalyst, J. Phys. Chem. C. 120 (2016) 18075–18087.

[137] E. Grau, A. Lesage, S. Norsic, C. Copéret, V. Monteil, P. Sautet, Tetrahydrofuran in TiCl4/THF/MgCl2: a non-innocent ligand for supported ziegler–natta polymerization catalysts, ACS Catal. 3 (2013) 52–56.

[138] E.J. Arlman, P. Cossee, Ziegler-Natta Catalysis III. Stereospecific Polymerization of Propene with the Catalyst System TiCI3-AlEt3, J. Catal. 3 (1964) 99–104.

[139] P. Cossee, Ziegler-Natta catalysis I. Mechanism of polymerization of a-olefins with Ziegler-Natta catalysts, J. Catal 3 (1964) 80–88.

[140] T. Taniike, M. Terano, Coadsorption model for first-principle description of roles of donors in heterogeneous Ziegler-Natta propylene polymerization, J. Catal. 293 (2012) 39–50.

[141] G. Takasao, T. Wada, A. Thakur, P. Chammingkwan, M. Terano, T. Taniike, Insight into structural distribution of heterogeneous Ziegler–Natta catalyst from non-empirical structure determination, J. Catal. 394 (2021) 299–306.

[142] M. Milanesi, A. Piovano, T. Wada, J. Zarupski, P. Chammingkwan, T. Taniike, E. Groppo, Influence of the synthetic procedure on the properties of three Ziegler-Natta catalysts with the same 1,3-diether internal donor, Catal. Today 418 (2023), 114077.

[143] A. Piovano, M. Signorile, L. Braglia, P. Torelli, A. Martini, T. Wada, G. Takasao, T. Taniike, E. Groppo, Electronic Properties of Ti Sites in Ziegler–Natta Catalysts, ACS Catal. 11 (2021) 9949–9961.

[144] T. Wada, A. Thakur, P. Chammingkwan, M. Terano, T. Taniike, A. Piovano, E. Groppo, Structural Disorder of Mechanically Activated δ-MgCl2 Studied by Synchrotron X-ray Total Scattering and Vibrational Spectroscopy, in: Catalysts, 2020.

[145] L. Noristi, P.C. Barbè, G. Baruzzi, Effect of the internal/external donor pair in high-yield catalysts for propylene polymerization, 1, Catal. -cocatalyst Interact., Makromol. Chem. 192 (1991) 1115–1127.

[146] L. Brambilla, G. Zerbi, S. Nascetti, F. Piemontesi, G. Morini, Experimental and Calculated Vibrational Spectra and Structure of Ziegler-Natta Catalyst Precursor: 50/1 Comilled MgCl2-TiCl4, Macromol. Symp. 213 (2004) 287–301.

[147] K. Soga, M. Ohgizawa, T. Shiono, Copolymerization of ethylene and propene with a TiCl4/MgCl2-Al(C2H5)3 catalyst system using a stopped-flow method, Makromol. Chem. 194 (1993) 2173–2181.

[148] J.C.J. Bart, Activation of Magnesium Chloride by Dry Milling, J. Mater. Sci. 28 (1993) 278–284.

[149] P. Galli, P.C. Barbé, G. Guidetti, R. Zannetti, A. Marigo, M. Bergozza, A. Fichera, The activation of MgCl2-supported Ziegler-Natta catalysts: A structural investigation, Eur, Polym. Chem. 19 (1983) 19–24.

[150] U. Giannini, E. Albizzati, S. Parodi, F. Pirinoli, Catalysts for polymerizing olefins, in, 1978.

[151] W. Phiwkliang, B. Jongsomjit, P. Praserthdam, Effect of ZnCl2- and SiCl4-doped TiCl4/MgCl2/THF catalysts for ethylene polymerization, J. Appl. Polym. Sci. 130 (2013) 1588–1594.

[152] A. Dashti, A. Ramazani Sa, Y. Hiraoka, S.Y. Kim, T. Taniike, M. Terano, Kinetic and morphological study of a magnesium ethoxide-based Ziegler–Natta catalyst for propylene polymerization, Polym. Int. 58 (2009) 40–45.

[153] D.H. Lee, Y.T. Jeong, K. Soga, In situ formation of magnesium chloride support and internal donor during preparation of propylene polymerization catalysts, Ind. Eng. Chem. Res. 31 (1992) 2642–2647.

[154] T. Funako, P. Chammingkwan, T. Taniike, M. Terano, Alternation of pore architecture of ziegler-natta catalysts through modification of magnesium ethoxide, Macromol. React. Eng. 9 (2015) 325–332.

[155] R.J.H. Clark, D. Lewis, D.J. Machin, R.S. Nyholm, Complexes of titanium trichloride, J. Chem. Soc. (1963) 379–387.

[156] R.J.H. Clark, Diffuse reflectance spectra of some anhydrous transition-metal halides, J. Chem. Soc. 0 (1964) 417–425.

[157] G. Pollini, I. Pollini, G. Spinolo, Optical Properties of α- and β-TiCl3, Phys. Stat. Sol. 27 (1968) 95–100.

[158] F. Cavallone, I. Pollini, G. Spinolo, Optical Properties of α-TiCl3 at the Magnetic Transition Temperature, Phys. Status Solidi B 45 (1971) 405–410.

[159] I. Pollini, Electronic transitions in alpha and beta titanium trichloride, Solid State Commun. 47 (1983) 403–408.

[160] C.H. Maulet, J.N. Tothill, P. Strange, J.A. Wilson, An optical investigation into the 3d^1 and 3d^2 transition-metal halides and oxyhalides, compounds near to delocalisation, J. Phys. C: Solid State Phys. 21 (1988) 2153–2179.

[161] C. Castán-Guerrero, D. Krizmancic, V. Bonanni, R. Edla, A. Deluisa, F. Salvador, G. Rossi, G. Panaccione, P. Torelli, A reaction cell for ambient pressure soft x-ray absorption spectroscopy, Rev. Sci. Instr. 89 (2018), 054101.

[162] D.H. Simonne, A. Martini, M. Signorile, A. Piovano, L. Braglia, P. Torelli, E. Borfecchia, G. Ricchiardi, THORONDOR: a software for fast treatment and analysis of low-energy XAS data, J. Synchrotron Radiat. 27 (2020) 1741–1752.

[163] F.M.F. De Groot, J.C. Fuggle, B.T. Thole, G.A. Sawatzky, L2,3 x-ray-absorption edges of d0 compounds: K+, Ca2+, Sc3+, and Ti4+ in Oh (octahedral) symmetry, Phys. Rev. B 41 (1990) 928–937.

[164] G. Takasao, T. Wada, A. Thakur, P. Chammingkwan, M. Terano, T. Taniike, Machine Learning-Aided Structure Determination for TiCl4–Capped MgCl2 Nanoplate of Heterogeneous Ziegler–Natta Catalyst, ACS Catal. 9 (2019) 2599–2609.

[165] J. Zarupski, A. Piovano, M. Signorile, A. Amodio, L. Olivi, C. Hendriksen, N. H. Friederichs, E. Groppo, Silica-magnesium-titanium Ziegler-Natta catalysts. Part 1: Structure of the pre-catalyst at a molecular level, J. Catal. 424 (2023) 236–245.

[166] J. Zarupski, A. Piovano, M.J. Werny, A. Martini, L. Braglia, P. Torelli, C. Hendriksen, N.H. Friederichs, F. Meirer, B.M. Weckhuysen, E. Groppo, Silica-magnesium-titanium Ziegler–Natta catalysts. Part II. Properties of the active sites and fragmentation behaviour, J. Catal. 423 (2023) 10–18.

[167] D. Cicmil, J. Meeuwissen, A. Vantomme, J. Wang, I.K. Van Ravenhorst, H.E. Van Der Bij, A. Muñoz-Murillo, B.M. Weckhuysen, Polyethylene with Reverse Co-monomer Incorporation: From an Industrial Serendipitous Discovery to Fundamental Understanding, Angew. Chem. Int. Ed. 54 (2015) 13073–13079.

[168] H. Liu, Y. Fang, H. Nakatani, M. Terano, Surface physico-chemical state of CO-prereduced Phillips CrO x/SiO2 catalyst and unique polymerization behavior in the presence of Al-alkyl cocatalyst, in: Macromolecular Symposia, 2004, pp. 37–46.

[169] B. Liu, P. Šindelář, Y. Fang, K. Hasebe, M. Terano, Correlation of oxidation states of surface chromium species with ethylene polymerization activity for Phillips CrOx/SiO2 catalysts modified by Al-alkyl, cocatalyst, J. Mol. Catal. A: Chem. 238 (2005) 142–150.

[170] W. Xia, K. Tonosaki, T. Taniike, M. Terano, T. Fujitani, B.P. Liu, Copolymerization of ethylene and cyclopentene with the phillips CrOx/SiO2 catalyst in the presence of an aluminum alkyl cocatalyst, J. Appl. Polym. Sci. 111 (2009) 1869–1877.

[171] G.A. Martino, A. Piovano, C. Barzan, S. Bordiga, E. Groppo, The effect of al-alkyls on the Phillips catalyst for ethylene polymerization: the case of diethylaluminum ethoxide (DEALE), Top. Catal. 61 (2018) 1465–1473.

[172] G.A. Martino, A. Piovano, C. Barzan, J. Rabeah, G. Agostini, A. Brueckner, G. Leone, G. Zanchin, T. Monoi, E. Groppo, Rationalizing the effect of triethylaluminum on the Cr/SiO2 Phillips catalysts, ACS, Catalysis 10 (2020) 2694–2706.

[173] D. Cicmil, J. Meeuwissen, A. Vantomme, B.M. Weckhuysen, Real-time Analysis of a Working Triethylaluminium-Modified Cr/Ti/SiO2 Ethylene Polymerization Catalyst with In Situ Infrared Spectroscopy, ChemCatChem 8 (2016) 1937–1944.

[174] D. Cicmil, I.K. Van Ravenhorst, J. Meeuwissen, A. Vantomme, B.M. Weckhuysen, Structure-performance relationships of Cr/Ti/SiO2 catalysts modified with TEAl for oligomerisation of ethylene: Tuning the selectivity towards 1-hexene, Catal. Sci. Tech. 6 (2016) 731–743.

[175] M.K. Jongkind, T. van Kessel, M.E.Z. Velthoen, N. Friederichs, B.M. Weckhuysen, Tuning the Redox Chemistry of a Cr/SiO2 Phillips Catalyst for Controlling

[176] M.K. Jongkind, F. Meirer, K.W. Bossers, I.C. ten Have, H. Ohldag, B. Watts, T. van Kessel, N. Friederichs, B.M. Weckhuysen, Influence of Metal-Alkyls on Early-Stage Ethylene Polymerization over a Cr/SiO2 Phillips Catalyst: A Bulk Characterization and X-ray Chemical Imaging Study, Chem. – A Eur. J. 27 (2021) 1688–1699.

[177] E. Groppo, A. Damin, C. Otero Arean, A. Zecchina, Enhancing the Initial Rate of Polymerisation of the Reduced Phillips Catalyst by One Order of Magnitude, Chem. Eur. J. 17 (2011) 11110–11114.

[178] T. Shiono, M. Ohgizawa, K. Soga, Reaction between carbon monoxide and a Ti-polyethylene bond with a MgCl2-supported TiCl4 catalyst system, Die Makromol. Chem. 194 (1993) 2075–2085.

[179] P.J.T. Tait, G.H. Zohuri, A.M. Kells, Comparative kinetic and active centre studies on magnesium chloride supported catalysts in propylene polymerization, Macromol. Symp. 89 (1995) 125–138.

[180] G.D. Bukatov, V.S. Goncharov, V.A. Zakharov, Interaction of ^{14}CO with Ziegler-type heterogeneous catalysts and effect of interaction products on the determination of the amount of active centers, Makromol. Chem. 187 (1986) 1041–1051.

[181] I. Tritto, M.C. Sacchi, P. Locatelli, On the insertion reaction of carbon oxides into metal-carbon bonds of Ziegler-Natta catalysts, Makromol. Chem. 4 (1983) 623–627.

[182] R. Cipullo, S. Mellino, V. Busico, Identification and count of the active sites in olefin polymerization catalysis by oxygen quench, Macromol. Chem. Phys. 215 (2014) 1728–1734.

[183] Y. Yu, R. Cipullo, C. Boisson, Alkynyl ether labeling: a selective and efficient approach to count active sites of olefin polymerization catalysts, ACS Catal. 9 (2019) 3098–3103.

[184] V. Busico, M. Guardasole, A. Margonelli, A.L. Segre, Insertion of Carbon Monoxide into Zr—Polymeryl Bonds: "Snapshots" of a Running Catalyst, J. Am. Chem. Soc. 122 (2000) 5226–5227.

[185] Z.-q Fan, L.-X. Feng, S.-L. Yang, Distribution of active centers on TiCl4/MgCl2 catalyst for olefin polymerization, J. Polym. Sci. A 34 (1996) 3329–3335.

[186] E.S. Cueny, H.C. Johnson, B.J. Anding, C.R. Landis, Mechanistic Studies of Hafnium-Pyridyl Amido-Catalyzed 1-Octene Polymerization and Chain Transfer Using Quench-Labeling Methods, J. Am. Chem. Soc. 139 (2017) 11903–11912.

[187] A. Piovano, J. Zarupski, E. Groppo, Disclosing the Interaction between Carbon Monoxide and Alkylated Ti^{3+} Species: a Direct Insight into Ziegler–Natta Catalysis, J. Phys. Chem. Lett. 11 (2020) 5632–5637.

[188] M.J. Werny, J. Zarupski, I.C. ten Have, A. Piovano, C. Hendriksen, N. H. Friederichs, F. Meirer, E. Groppo, B.M. Weckhuysen, Correlating the Morphological Evolution of Individual Catalyst Particles to the Kinetic Behavior of Metallocene-Based Ethylene Polymerization Catalysts, JACS Au 1 (2021) 1996–2008.

[189] L. Resconi, L. Cavallo, A. Fait, F. Piemontesi, Selectivity in propene polymerization with metallocene catalysts, Chem. Rev. 100 (2000) 1253–1345.

[190] J.A. Ewen, L. Haspeslach, J.L. Atwood, H. Zhang, Crystal structures and stereospecific propylene polymerizations with chiral hafnium metallocene catalysts, J. Am. Chem. Soc. 109 (1987) 6544–6545.

[191] B. Rieger, C. Troll, J. Preuschen, Ultrahigh molecular weight polypropene elastomers by high activity "Dual-Side" hafnocene catalysts, Macromolecules 35 (2002) 5742–5743.

[192] A. Laine, M. Linnolahti, T.A. Pakkanen, J.R. Severn, E. Kokko, A. Pakkanen, Comparative Theoretical Study on Homopolymerization of α-Olefins by Bis (cyclopentadienyl) Zirconocene and Hafnocene: Elemental Propagation and Termination Reactions between Monomers and Metals, Organometallics 29 (2010) 1541–1550.

[193] M.R. Machat, A. Fischer, D. Schmitz, M. Vöst, M. Drees, C. Jandl, A. Pöthig, N.P. M. Casati, W. Scherer, B. Rieger, 4 Metallocene Catalysis: Examination of the Metal–Carbon Bond (Behind the Scenes of Group), Organometallics 37 (2018) 2690–2705.

[194] A. Vittoria, G.P. Goryunov, V.V. Izmer, D.S. Kononovich, O.V. Samsonov, F. Zaccaria, G. Urciuoli, P.H.M. Budzelaar, V. Busico, A.Z. Voskoboynikov, D. V. Uborsky, C. Ehm, R. Cipullo, Hafnium vs. Zirconium, the perpetual battle for supremacy in catalytic olefin polymerization: A simple matter of electrophilicity? Polymers 13 (2021).

[195] V. Busico, R. Cipullo, R. Pellecchia, G. Talarico, A. Razavi, Hafnocenes and MAO: Beware of Trimethylaluminum!, Macromolecules 42 (2009) 1789–1791.

[196] C. Ehm, R. Cipullo, P.H.M. Budzelaar, V. Busico, Role(s) of TMA in polymerization, Dalton Trans. 45 (2016) 6847–6855.

[197] C. Morterra, M. Peñarroya Mentruit, G. Cerrato, Acetonitrile adsorption as an IR spectroscopic probe for surface acidity/basicity of pure and modified zirconias, Phys. Chem. Chem. Phys. 4 (2002) 676–687.

[198] M. Bochmann, L.M. Wilson, Synthesis and insertion reactions of cationic alkylbis (cyclopentadienyl)titanium complexes, J. Chem. Soc., Chem. Commun. (1986) 1610–1611.

[199] R.F. Jordan, C.S. Bajgur, W.E. Dasher, A.L. Rheingold, Hydrogenation of cationic dicyclopentadienylzirconium(IV) alkyl complexes. Characterization of cationic zirconium(IV) hydrides, Organometallics 6 (1987) 1041–1051.

[200] M. Bochmann, L.M. Wilson, M.B. Hursthouse, M. Motevalli, Insertion reactions of nitriles in cationic alkylbis(cyclopentadienyl)titanium complexes: the facile synthesis of azaalkenylidene titanium complexes and the crystal and molecular structure of [(indenyl)2Ti(NCMePh)(NCPh)]BPh4, Organometallics 7 (1988) 1148–1154.

[201] C. Barzan, D. Gianolio, E. Groppo, C. Lamberti, V. Monteil, E.A. Quadrelli, S. Bordiga, The effect of hydrosilanes on the active sites of the phillips catalyst: The secret for in situ α-olefin generation, Chem. - A Eur. J. 19 (2013) 17277–17282.

[202] C. Barzan, E. Groppo, E.A. Quadrelli, V. Monteil, S. Bordiga, Ethylene polymerization on a SiH 4-modified Phillips catalyst: Detection of in situ produced α-olefins by operando FT-IR spectroscopy, Phys. Chem. Chem. Phys. 14 (2012) 2239–2245.

[203] G.A. Martino, A. Piovano, C. Barzan, Y.-K. Liao, E. Morra, K. Hirokane, M. Chiesa, T. Monoi, E. Groppo, Cr[CH(SiMe3)2]3/SiO2 catalysts for ethene polymerization: The correlation at a molecular level between the chromium loading and the microstructure of the produced polymer, J. Catal. 394 (2021) 131–141.

[204] H. Ikeda, T. Monoi, Y. Sasaki, Performance of the Cr[CH(SiMe3)2]3/SiO2 catalyst for ethylene polymerization compared with the performance of the phillips catalyst, J. Polym. Sci. A Polym. Chem. 41 (2003) 413–419.

[205] T. Monoi, H. Ikeda, Y. Sasaki, Y. Matsumoto, Ethylene polymerization with silica-supported Cr[CH(SiMe3)2]3 catalyst. effect of silica calcination temperature and Cr content, Polym. J. 35 (2003) 608–611.

[206] A. Piovano, E. Morra, M. Chiesa, E. Groppo, Tuning the Ti3+ and Al3+ Synergy in an Al2O3/TiClx Catalyst to Modulate the Grade of the Produced Polyethylene, ACS Catal. 7 (2017) 4915–4921.

[207] A. Piovano, K.S. Thushara, E. Morra, M. Chiesa, E. Groppo, Unraveling the catalytic synergy between Ti3+ and Al3+ sites on a chlorinated Al2O3: a tandem approach to branched polyethylene, Angew. Chem. Int. Ed. 55 (2016) 11203–11206.